Hindawi Publishing Corporation
Advances in High Energy Physics
Volume 2013, Article ID 460123, 35 pages
http://dx.doi.org/10.1155/2013/460123

Review Article

Future Long-Baseline Neutrino Facilities and Detectors

Milind Diwan,[1] Rob Edgecock,[2] Takuya Hasegawa,[3] Thomas Patzak,[4] Masato Shiozawa,[5] and Jim Strait[6]

[1] *Physics Department, Brookhaven National Laboratory, Upton, NY 11973, USA*
[2] *University of Huddersfield and STFC Rutherford Appleton Laboratory, Didcot OX11 0QX, UK*
[3] *High Energy Accelerator Research Organization (KEK), Tsukuba, Ibaraki 305-0801, Japan*
[4] *AstroParticule et Cosmologie (APC), Université Paris Diderot, CNRS/IN2P3, CEA/Irfu, Observatoire de Paris, Sorbonne Paris Cité, 10 rue Alice Domon et Léonie Duquet, 75205 Paris Cedex 13, France*
[5] *Kamioka Observatory, Institute for Cosmic Ray Research, University of Tokyo, Kamioka, Gifu 506-1205, Japan*
[6] *Fermi Accelerator National Laboratory, Batavia, IL 60510, USA*

Correspondence should be addressed to Thomas Patzak; patzak@apc.univ-paris7.fr

Received 25 June 2012; Revised 12 October 2012; Accepted 24 October 2012

Academic Editor: Koichiro Nishikawa

Copyright © 2013 Milind Diwan et al. This is an open access article distributed under the Creative Commons Attribution License, which permits unrestricted use, distribution, and reproduction in any medium, provided the original work is properly cited.

We review the ongoing effort in the US, Japan, and Europe of the scientific community to study the location and the detector performance of the next-generation long-baseline neutrino facility. For many decades, research on the properties of neutrinos and the use of neutrinos to study the fundamental building blocks of matter has unveiled new, unexpected laws of nature. Results of neutrino experiments have triggered a tremendous amount of development in theory: theories beyond the standard model or at least extensions of it and development of the standard solar model and modeling of supernova explosions as well as the development of theories to explain the matter-antimatter asymmetry in the universe. Neutrino physics is one of the most dynamic and exciting fields of research in fundamental particle physics and astrophysics. The next-generation neutrino detector will address two aspects: fundamental properties of the neutrino like mass hierarchy, mixing angles, and the CP phase, and low-energy neutrino astronomy with solar, atmospheric, and supernova neutrinos. Such a new detector naturally allows for major improvements in the search for nucleon decay. A next-generation neutrino observatory needs a huge, megaton scale detector which in turn has to be installed in a new, international underground laboratory, capable of hosting such a huge detector.

1. International Context and Motivation

For many decades, research on the properties of neutrinos and the use of neutrinos to study the fundamental building blocks of matter has unveiled new, unexpected laws of nature. In the basic version of the standard model of particle physics, neutrinos enter as massless, neutral, spin one-half particles. Left-handed neutrinos form an electroweak isospin doublet with their charged, massive partners, electrons, muons, and taus. The right-handed neutrinos form an electroweak isospin singlet. Today, we have strong experimental evidence that neutrinos have a nonvanishing mass and that they change flavor while propagating in space. This phenomenon is called neutrino oscillations. These experimental observations imply an extension of the standard model and point to a more general formalism. Up to now, no other experimentally proven indication for physics beyond the standard model has been found with accelerator-based experiments at LEP, the Tevatron, and LHC. The search for neutrino oscillations has been triggered by astrophysics experiments with neutrinos, namely, the observation of neutrinos from the Sun and, later on, neutrinos generated in the interaction of cosmic rays with the Earth's atmosphere: atmospheric neutrinos. At the same time solar neutrino spectroscopy allows a much better understanding and theoretical description of our star. The detection of a handful of neutrinos from a supernova in 1987 by the Kamiokande and IMB experiments gave a fundamental input and verification of supernova models. Over the last few decades, the results of neutrino experiments have triggered a tremendous amount of development in

theory: theories beyond the standard model or at least extensions of it, development of the standard solar model and modeling of supernova explosions as well as the development of theories to explain the matter-antimatter asymmetry in the universe.

Today, the common way of describing neutrino oscillations is the following.

The neutrinos ν_e, ν_μ, and ν_τ are weak eigenstates while the mass eigenstates ν_i are related to the weak eigenstates ν_l via a neutrino mixing matrix:

$$\left|\nu_l\right\rangle = \sum_i U_{li}^{\star} \left|\nu_i\right\rangle . \tag{1}$$

The coefficients U_{il} form a matrix, called MNSP (Maki, Nakagawa, Sakata, Pontecorvo):

$$\begin{pmatrix} \nu_e \\ \nu_\mu \\ \nu_\tau \end{pmatrix} = \begin{pmatrix} U_{e1} & U_{e2} & U_{e3} \\ U_{\mu 1} & U_{\mu 2} & U_{\mu 3} \\ U_{\tau 1} & U_{\tau 2} & U_{\tau 3} \end{pmatrix} \begin{pmatrix} \nu_1 \\ \nu_2 \\ \nu_3 \end{pmatrix}. \tag{2}$$

The MNSP matrix can be parametrized in three *mixing angles*, θ_{12}, θ_{23}, θ_{13}, and a complex phase δ, called the CP phase:

$$\begin{pmatrix} 1 & 0 & 0 \\ 0 & c_{23} & s_{23} \\ 0 & -s_{23} & c_{23} \end{pmatrix} \begin{pmatrix} c_{13} & 0 & s_{13}e^{-i\delta} \\ 0 & 1 & 0 \\ -s_{13}e^{i\delta} & 0 & c_{13} \end{pmatrix} \begin{pmatrix} c_{12} & s_{12} & 0 \\ -s_{12} & c_{12} & 0 \\ 0 & 0 & 1 \end{pmatrix}, \tag{3}$$

where s_{ij} and c_{ij} are, respectively, $\sin\theta_{ij}$ and $\cos\theta_{ij}$, with $i, j = (1, 2, 3)$. Using this parameterization, we can calculate the probability for a neutrino with fixed flavor ν_α to oscillate to a different weak eigenstate, ν_β after a time t. This probability that a neutrino ν_α after a time t changes flavor to β is expressed as

$$P_{\nu_\alpha \to \nu_\beta}(t) = \left|\left\langle \nu_\beta \mid \nu_\alpha(t)\right\rangle\right|^2, \tag{4}$$

where

$$\left|\nu_l(t)\right\rangle = \sum_i U_{\alpha i}^{\star} e^{-i(E_i t/\hbar)} \left|\nu_i\right\rangle , \tag{5}$$

and the $U_{\alpha i}^{\star}$ are the coefficient of the MNSP matrix. It follows

$$P_{\nu_\alpha \to \nu_\beta}(t) = \left|\left\langle \sum_i U_{\alpha i}^{\star} e^{-i(E_i t/\hbar)} U_{\beta i} \right\rangle\right|^2. \tag{6}$$

Developing the above equation leads to the probability expressed as

$$P_{\nu_\alpha \to \nu_\beta}(t) = \delta_{\alpha\beta} - 4\sum_{k>j} U_{\alpha i}^{\star} U_{\beta i} U_{\alpha j} U_{\beta j}^{\star} \sin^2\left(\frac{\left(E_k - E_j\right)t}{2\hbar}\right). \tag{7}$$

We can write t as L/c and rewrite the energy differences as

$$\left(E_k - E_j\right)\frac{t}{\hbar} = \left(E_k - E_j\right)\frac{L}{c\hbar} \sim \frac{c^4 L}{2\hbar c \cdot pc}\left(m_i^2 - m_k^2\right). \tag{8}$$

Using the notation $\Delta m_{ki}^2 = (m_k^2 - m_i^2)c^4$ and the approximation of relativistic neutrinos ($E \gg mc^2$), the previous equation becomes

$$P_{\nu_\alpha \to \nu_\beta} = \delta_{\alpha\beta} - 4\sum_{k>j} U_{\alpha i}^{\star} U_{\beta i} U_{\alpha j} U_{\beta j}^{\star} \sin^2\left(\frac{\Delta m_{ki}^2 L}{4E}\right). \tag{9}$$

This expression of the probability is exact for neutrino oscillations in vacuum.

It is important to remark that neutrino oscillation experiments have no access to the absolute neutrino mass. On the other hand, they are a powerful instrument to have information on the mass square differences:

$$\Delta m_{ij}^2 = m_j^2 - m_i^2. \tag{10}$$

It is evident that only two mass square differences are independent from each other:

$$\left(m_2^2 - m_1^2\right) + \left(m_3^2 - m_2^2\right) + \left(m_1^2 - m_3^2\right) = 0, \tag{11}$$

so, the measure of the Δm_{12}^2 and the Δm_{23}^2 is enough to constrain the system.

According to the sign of Δm_{32}^2, there are two possible mass hierarchies:

(i) $\Delta m_{23}^2 > 0$: normal hierarchy (NH). In this situation, we have $m_3 > m_2 > m_1$. This case seems to be the more natural, as the lightest neutrinos would turn to be the ν_e, as the electron is lighter than the μ and τ;

(ii) $\Delta m_{23}^2 < 0$: inverted hierarchy (IH). In this situation, m_3 would be the lightest neutrino.

In this paper, we will use the definition of the observables from above to describe the physics case of the proposed new long-baseline experiments.

The above-mentioned examples make neutrinos physics one of the most dynamic and exciting fields of research in fundamental particle physics and astrophysics. The next-generation neutrino detector will address two aspects: fundamental properties of the neutrino like mass hierarchy, mixing angles and the CP phase, and low-energy neutrino astronomy with solar, atmospheric, and supernova neutrinos. Such a new detector naturally allows for major improvements in the search for nucleon decay. A next-generation neutrino observatory needs a huge, megaton scale detector which in turn has to be installed in a new, international underground laboratory, capable of hosting such a huge detector.

In the US, the strategy for a future long-baseline experiment has been under development over the last decade. The scientific goals of a future US-based long-baseline neutrino project have been discussed and reviewed extensively by the US National Research Council and the Particle Physics Advisory Panels. The National Research Council reports in 2003 and 2011 have endorsed a project with a large capability underground detector located at a distance of >1000 km from Fermilab.

In Europe, a roadmap has been established in 2008 and updated in 2011 by ASPERA (AStroParticle ERAnet).

In the 2011 update one can read *"The goals of a megaton scale detector as addressed by the design studies LAGUNA range from low energy neutrino astrophysics (e.g., supernova, solar, geo and atmospheric neutrinos) to fundamental searches without accelerators (e.g., search for proton decay) and accelerator driven physics (e.g., observation of CP violation). Due to its high cost, the program can be developed only in a global context."* The recent confirmation of a nonzero mixing angle θ_{13} permits a series of very exciting measurements for neutrino mass hierarchy and CP violation using CERN beams. In Europe, there are three ongoing FP7 design studies: LAGUNA, Large Apparatus studying Grand Unification and Neutrino Astrophysics (Grant Agreement no. 212343, FP7-INFRA-2007-1), EUROnu (Grant Agreement no. 212372), and LAGUNA-LBNO, Large Apparatus studying Grand Unification and Neutrino Astrophysics and Long Baseline Neutrino Oscillations (Grant Agreement no. 284518, FP7-INFRA-2011-2.1.1.).

In Japan, projects exploring the lepton sector CP symmetry both with a 100 kt detector based on a liquid Argon time projection chamber and a 560 kt water Cherenkov detector (Hyper-Kamiokande) are being planned [1, 2]. In both scenarios, a high-intensity neutrino beam would be provided by J-PARC.

As shown above, there is a worldwide consensus among physicists on the scientific priorities and the next-generation neutrino detector and infrastructure. One can also see the very strong competition between different countries to host such observatory for the next 30 to 50 years.

2. The US Long-Baseline Neutrino Program

The US accelerator neutrino program at Fermilab consists of a diverse set of experiments with intense neutrinos beams. The Fermilab Main Injector with the NuMI neutrino beamline operates at 350 kW with a tunable neutrino beam covering from 0.5 GeV to 10 GeV, and the neutrino beamline from the 8 GeV Booster accelerator (BNB) operates with a low-energy neutrino beam covering from 0.2 GeV to 1 GeV. The current and near future program is listed as follows: the MINOS experiment is a 5 kt magnetized steel/scintillator detector operating in the NuMI beamline at a baseline of 735 km. The main goals of MINOS consist in the measurement of muon neutrino disappearance and the parameters that govern atmospheric neutrino oscillations [3]. The NOvA experiment is a totally active segmented liquid scintillation detector located off-axis (14 mrad) at a distance of 810 km from the NuMI target. The physics goal of NOvA is the measurement of muon to electron neutrino conversion [4] and the parameters that govern the electron appearance mode. The MINERVA experiment which will perform precision measurements of neutrino cross-sections is also located in the NuMI beamline on-site at Fermilab in an underground cavern [5]. The MiniBooNe experiment (Mineral Oil Cherenkov detector) [6] is in the low-energy neutrino beamline that uses protons from the Fermilab 8 GeV booster. The MicroBooNe experiment (liquid argon TPC) [7] will also be located in the booster neutrino beamline. The MiniBooNe and MicroBooNe experiments are exploring the short baseline neutrino oscillation anomalies [8].

The strategy for a future long-baseline experiment in the US has been under development over the last decade [9–12]. The scientific goals of a future US-based long-baseline neutrino project have been discussed and reviewed extensively by the US National Research Council and the Particle Physics Advisory Panels. The National Research Council reports in 2003 and 2011 [13, 14] have endorsed a project with a large capability underground detector located at a distance of >1000 km from Fermilab. Furthermore, the NUSAG report in 2007 [15] and the P5 report in 2008 [16] considered the scientific benefits of a long-baseline experiment with a baseline of ~1300 km with a capable detector, either a water Cherenkov or a liquid argon TPC located deep in the former Homestake mine in Lead, SD, USA. As a consequence of these reports which constitute a consensus in the US particle physics community, the US Department of Energy funded the development of the long-baseline neutrino experiment (LBNE) with a goal of having a next-generation large detector located at a distance of 1300–1500 km in an intense broadband accelerator neutrino beam. With the recent discovery of the value of θ_{13} [17], the LBNE program is scientifically highly motivated.

The long-baseline neutrino experiment (LBNE) is the next major planned neutrino program in the US. The experiment as currently envisioned comprises a new 700 kW beamline at Fermilab, whose spectrum is optimized for this physics and which is upgradable to handle more than 2 MW of beam power from the future high-intensity proton accelerator (named the Project-X upgrade [18]); a near detector complex to fully characterize the unoscillated beam and a large far detector at the Homestake mine in South Dakota, at a baseline of 1,300 km, to make precision measurements of neutrino oscillation phenomena and enable a broad program of nonaccelerator-based physics. The detector envisioned at the Homestake site is either a Water Cherenkov detector with a total fiducial mass of 200 kt or a liquid argon time projection chamber with a fiducial mass of 34 kt. The beam designed will be a horn-focused broadband beam with an energy spectrum from 0.5 GeV to 5 GeV and a mean energy near 2.5 GeV. The technical design for LBNE has been extensively documented in a draft Conceptual Design Report [19]. In the following sections, we will briefly review some of the technical details of the LBNE design.

2.1. Technical Design for LBNE

2.1.1. Beam Design for LBNE. The LBNE beam design is a conventional, horn-focused neutrino beamline. The components of the beamline will be designed to extract a proton beam from the Fermilab Main Injector (MI) and transport it to a target area where the collisions generate a beam of charged particles that decay in a decay pipe. The facility is designed for initial operation at proton-beam power of 700 kW, with the capability to support an upgrade to 2.3 MW. In the reference design, extraction of the proton beam occurs at MI-10, a new installation on the Main Injector accelerator. After extraction, this primary beam establishes a horizontally

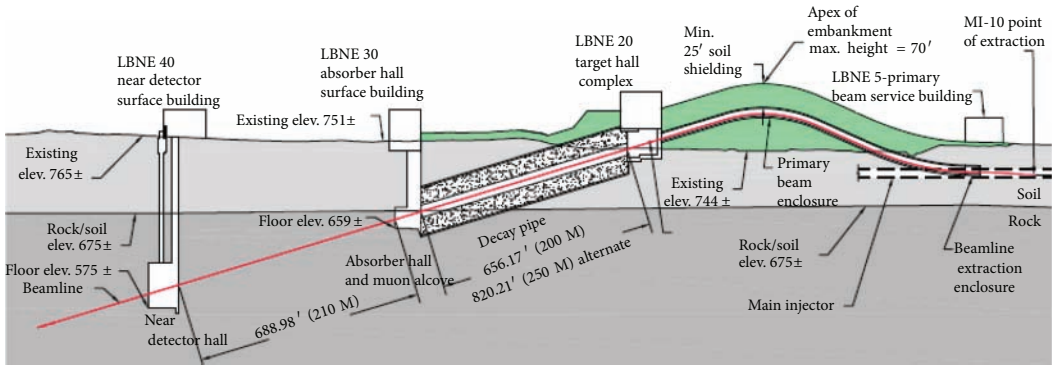

Figure 1: Schematic view of the LBNE beam design located at Fermilab.

straight heading west-northwest toward the far detector, but will be bent upward to an apex before being bent downward at the appropriate angle, 101 milliradians (5.79°) as shown in Figure 1. The primary beam will be above grade for about ~210 meters; this design minimizes expensive underground construction and significantly enhances capability for groundwater radiological protection. The design requires, however, construction of an earthen embankment, or hill, whose dimensions are commensurate with the bending strength of the dipole magnets required for the beamline. The embankment will need to be approximately 335 m long and 20 m high above grade at its peak.

The target marks the transition from the intense, narrowly directed proton beam to the more diffuse, secondary beam of particles that in turn decay to produce the neutrino beam. After collection and focusing, the pions and kaons need a long, unobstructed volume in which to decay. This decay volume in the LBNE reference design is a pipe of circular cross-section with its diameter (4 meters) and length (200 meters) optimized such that decays of the pions and kaons result in neutrinos in the energy range useful for the experiment. The decay volume is followed immediately by the absorber, which removes the remaining beam hadrons.

The experience gained from the various neutrino projects at FNAL has been employed extensively in the LBNE beamline conceptual design. In particular, the NuMI beamline serves as the prototype design. Nevertheless, the LBNE beamline contains considerable innovation with regards to simplicity of construction and radiological protection.

The reference design for the primary beam and the neutrino beam is suitable for the initial beam power of ~700 kW in all respects. Some aspects of the reference design are also appropriate for a beam power of ≥2.3 MW. These include the radiological shielding and the size of the underground enclosures as well as systems such as the beam absorber and the remote handling, which cannot be upgraded after exposure to a high-intensity beam. Some aspects of the reference design are planned for a beam power upgrade to 2.3 MW. The underground enclosures will have the appropriate steel and concrete shielding required for future beam upgrades.

2.1.2. Event Rate. The LBNE beamline is expected to initially use ~700 kW of proton power from the Main injector at an energy of 120 GeV (4.9×10^{13} protons per spill every 1.33 sec). The spill length is approximately 10 μsec. The beamline is designed to be able to run at a lower-energy proton beam of 60 GeV. Such flexibility can be used to reduce backgrounds from beam tails and change the beam spectrum for systematic studies in the future. A complete GEANT-based simulation of the beamline is used to evaluate the beam spectrum and expected numbers of events at a far detector at 1300 km. The expected muon neutrino charged current event rate superimposed on the $\nu_\mu \rightarrow \nu_e$ oscillation probability is shown in Figure 2. The beam is designed to give maximum event rate across the 0.5 to 5 GeV energy region with the constraint that the maximum beam power from the FNAL injector is available at 120 GeV. It should be noted that for the appearance mode the maximum of the probability shifts from below 2 GeV (normal hierarchy for neutrinos) to above 3 GeV (normal hierarchy for antineutrinos); furthermore, the broadband beam allows separation of the degeneracies evident in the Figure, for example, $\delta_{CP} = \pi/2, 0$ at ~1.8 GeV and $\delta_{CP} = -\pi/2, 0$ at ~4 GeV. With this beam design, the total charged current muon neutrino event rate per year in a 34 kt liquid argon (200 kt water Cherenkov) detector will be 6000 events (35000 events) without oscillations with approximately 0.7% contamination of electron neutrinos and 4% contamination of muon antineutrinos. The total charged current muon antineutrino event rate per year in a 34 kt liquid argon (200 kt water Cherenkov) detector will be 2200 events (13000 events) without oscillations with approximately 1% contamination of electron neutrinos and antineutrinos and 30% contamination of muon neutrinos. For the above calculation, the Fermilab Main Injector is assumed to run 2×10^7 sec per year.

2.1.3. Water Cherenkov Detector Design for LBNE. The LBNE water Cherenkov detector design consists of a very large excavated cavity in a very strong and stable rock formation at the 4850 ft level in the Homestake facility. The cylindrical cavity will be lined with a smooth liner and filled with extremely pure water. The reference design calls for a total water mass of 266 kt and a fiducial mass of 200 kt. PMTs will surround the fiducial volume on the top, bottom, and around the perimeter. The wall PMTs will be suspended by cables about half a meter from the inner surface of the liner. The top and floor PMTs will be mounted to the structural framework.

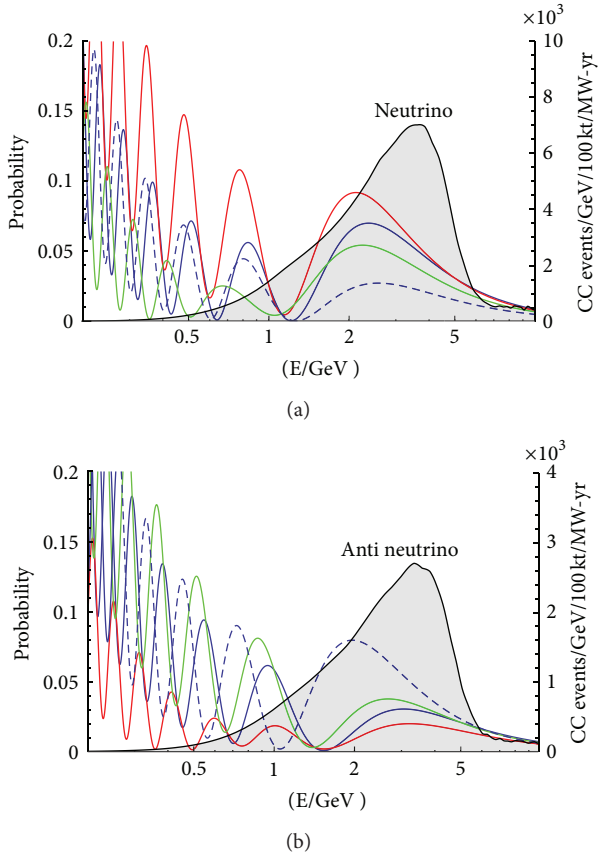

FIGURE 2: The muon charged current event rate in a 100 kt detector at 1300 km for neutrino (a) and antineutrino (b) running for the LBNE beam design with beam power of 700 kW and 2×10^7 sec (1 year of running) of running time. The event rate as a function of energy is superimposed on the expected $\nu_\mu \rightarrow \nu_e$ oscillation probability for $\theta_{13} = 9^\circ$. The various curves correspond to blue ($\delta_{CP} = 0$), blue-dashed ($\delta_{CP} = 0$ and inverted hierarchy), red ($\delta_{CP} = \pi/2$), and green ($\delta_{CP} = -\pi/2$).

Each PMT will be connected via cable to readout electronics on the balcony above the water detector. The baseline design includes a top veto region, which will consist of an array of horizontally oriented PMTs optically separated from the rest of the detector. The veto will be used to tag cosmic ray muons that enter the detector from above that form a background for astrophysical neutrino measurements.

Provisions will be made to fill the detector with purified water and to recycle this water through the purification system and cool it. There will be provision to periodically calibrate the detector and monitor its status and performance. Finally, there will be provisions to prevent radon contamination of the detector water.

The optimum shape of the detector from excavation considerations at the Homestake site in the Yates rock formation (an amphibolite formation with some rhyolite intrusions) is a vertical circular cylinder. There are two limitations on the maximum diameter: the light attenuation length in water (~90 meters) and the maximum rock excavation diameter that does not require extraordinary rock support. The studies of both the Large Cavity Advisory Board (composed of world experts in underground construction) and Golder Associates concluded that an excavated cylindrical cavity with a diameter of 65 meters was completely feasible and cost efficient.

The major detector components are (1) the water containment system, (2) the photomultiplier mounting, housing and cable system, (3) the electronics readout and trigger system, (4) calibration procedures, (5) the water purification and cooling system, and (6) event reconstruction and data analysis. Table 1 summarizes the important detector parameters. Figure 3 shows a schematic 3-dimensional view of the detector design as located at the 4850 ft level of the Homestake facility.

2.1.4. Liquid Argon Detector Design for LBNE. The LBNE LArTPC consists of two massive cryostats in a single cavern, oriented end-to-end along the beam direction (roughly east to west), and located at the 4850 level (4850 L) of the Homestake underground facility. The fiducial mass of each, as defined for neutrino oscillation studies, is 17 kt and the active (instrumented) mass is 20 kt, resulting in a total active mass of 40 kt. Figure 4 shows the proposed layout of the far site, and Figure 5 shows the detector configuration.

In an LArTPC, a uniform electric field is created within the TPC volume between cathode planes and anode wire planes. Charged particles passing through the TPC release ionization electrons that drift to the anode wire planes. The bias voltage is set on the anode plane wires so that ionization electrons drift between the first several (induction) planes and are collected on the last (collection) plane. Readout electronics amplify and continuously digitize the induced waveforms on the sensing wires at several MHz and transmit these data to the data acquisition (DAQ) system for processing. The wire planes are oriented at different angles allowing a 3D reconstruction of the particle trajectories. In addition to these basic components, a photon-detection system provides a trigger for proton decay and galactic supernova neutrino interactions.

The principal parameters of the LBNE liquid argon far detector are given in Table 2.

The LBNE liquid argon detector design is an extension of the successful ICARUS design; nevertheless, it has several innovative elements: the cryostat construction uses commercial stainless steel membrane technology engineered and produced by industry. These vessels are widely deployed in liquefied natural gas (LNG) tanker ships and tanks and are typically manufactured in sizes much larger than that of the LAr-FD. This is an inherently clean technology with passive insulation. The time projection chamber (TPC) is the active detection element of the LAr-FD. The TPC is located inside the cryostat vessel and is completely submerged in LAr at 89 K. Its active volume is 14 m high, 22.4 m wide, and 45.6 m long in the beam direction. It has four rows of cathode plane assemblies (CPAs) planes interleaved with three rows of anode plane assemblies (APAs) planes that are oriented vertically, parallel to the beamline, with the electric field applied perpendicular to the planes. The maximum electron-drift distance between a cathode and an adjacent

Table 1: A summary of the important water Cherenkov detector design parameters.

Detector design parameter	Value
Fiducial volume	200 kt (200,000 m^3)
Location	Homestake 4850 ft level
Shape	Right circular cylinder
Cylinder excavation dimensions	65.6 m diameter × 81.3 m height
Dome height	16 m
Vessel liner dimensions	65 m diameter × 80.3 m height
Water volume dimensions	65 m diameter × 79.5 m height
Total water volume	263,800 m^3
Distance from Neat line to PMT equator	0.85 m
Dimensions of instrumented volume	63.3 m diameter × 76.6 m height
Instrumented volume	241,000 m^3
Fiducial volume cut	2 m
Fiducial volume dimensions	59.3 m diameter × 72.6 m height
Number of PMTs	29,000
PMT diameter	12 in (304 mm)
Peak QE of PMTs (at 420 nm)	30%
PMT spectral response	300–650 nm
PMT transit time spread	2.7 ns
Light gain from light collectors	41%
Max water pressure on PMTs	7.9 bar
Number/type veto PMTs	200 × 12 in
Water fill rate	250 gal/min (0.95 m^3/min)
Detector fill time	195 days
Water circulation rate	1200 gal/min (4.5 m^3/min)
Water volume exchange time	~40 days
Water temperature	13°C
Electronics burst capability	>1 M events in 10 s
Electronics time resolution	<1 ns
Electronics dynamic range	1–1000 PE
Timing calibration	<1 ns
PMT pulse height calibration	<10%
Radon content	<1 mBq/m^3

anode is 3.7 m. Both the cathode and anode plane assemblies are 2.5 m wide and 7 m high. Two 7 m modules (either APA or CPA) stack vertically to instrument the 14 m active depth. In each row, 18 such stacks are placed edge-to-edge along the beam direction, forming the 45.6 m active length of the detector. Each cryostat houses a total of 108 APAs and 144 CPAs. A "field cage" surrounds the top and ends of the detector to ensure uniformity of the electric field. The field cage is assembled from panels of FR-4 sheets with parallel copper strips connected to resistive divider networks.

Each APA has three wire planes that are connected to readout electronics: two induction planes and one collection plane (X). A fourth wire plane, grid plane (G), is held at a bias voltage but is not instrumented with readout electronics. The gird plane improves the signal-to-noise ratio on the U plane and provides electrostatic discharge protection for the readout electronics. A key innovative feature of the LBNE LAR detector is the use of cold electronics. Requirements for low noise and for extreme purity of the LAr motivate locating the front-end electronics in the LAr (hence "cold electronics") close to the anode wires, which reduces the signal capacitance (thereby minimizing noise). The use of CMOS electronics in this application is particularly attractive since the series noise of this process has a noise minimum at 89 K. The large number of readout channels required to instrument the LAr-FD TPCs motivates the use of CMOS ASICs. Signal zero-suppression and multiplexing will be implemented in the ASIC, minimizing the number of cables and feedthroughs in the ullage gas, and therefore reducing contamination from cable outgassing.

Both detector designs for LBNE, the water Cherenkov and liquid argon, were reviewed extensively for cost, schedule, and scientific performance. The fiducial masses of both detectors were chosen to achieve similar performance for neutrino oscillation physics, in particular the sensitivity to CP violation. The reviews concluded that both detectors could achieve the performance goals for neutrino physics; nevertheless, there were some advantages to the liquid argon

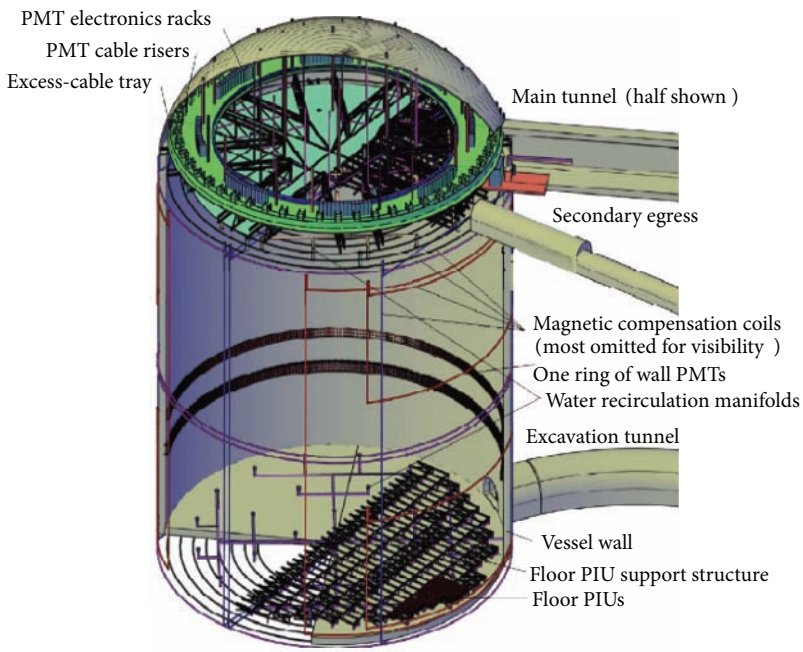

Figure 3: Schematic design of a 200 kt water Cherenkov detector in the Homestake underground facility.

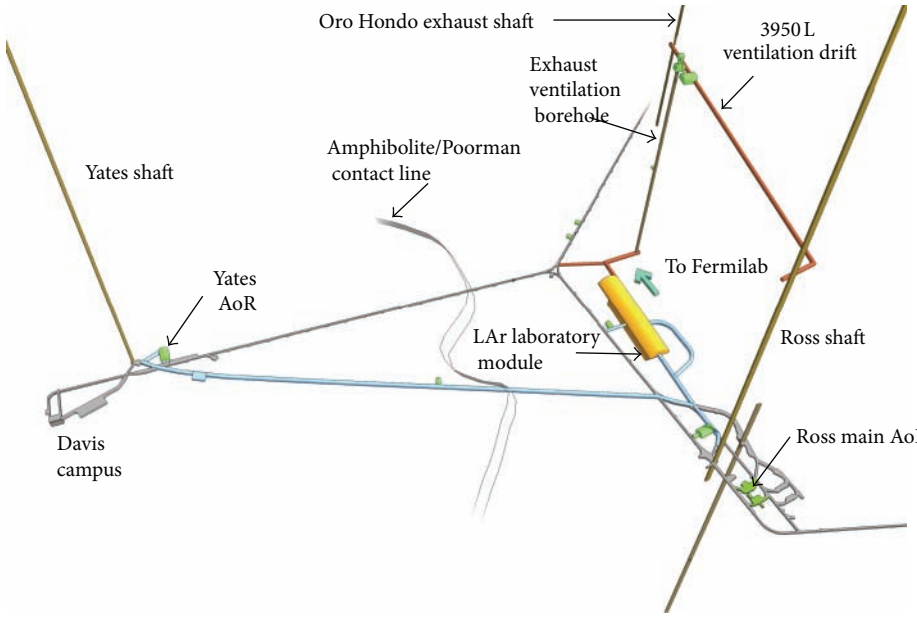

Figure 4: Location of LAr-FD at the 4850 L. Primary access to the upper level of the LAr-FD cavern is through a horizontal tunnel that connects to the Ross shaft. A second horizontal tunnel near the midpoint of the cavern provides secondary egress to the existing 4850 L tunnels. A decline tunnel to the lower level is used to remove waste rock during construction and serves as a secondary egress from the cryostat septum area during operations. Cavern supply air enters the cavern from the Ross shaft and exits through a new ventilation shaft that connects to the Oro Hondo.

detector due to its fine granularity. Liquid argon is also a complementary technology in terms of searching for proton decay and its sensitivity to low-energy electron neutrinos (instead of electron antineutrinos) from supernova. Furthermore, it was clearly cost-prohibitive to design and build both types of detectors; therefore, through an extensive process of selection, the liquid argon option was selected as the reference design for LBNE.

In addition to the far detector, the LBNE design also includes near detectors to monitor the neutrino beam before it leaves the Fermilab site. The set of detector systems for the near detectors reference design consists of a

Table 2: LAr-FD principal parameters.

Parameter	Value
Active (fiducial) mass	40 (33) kt
Location	Homestake 4850 ft level
Number of detector modules (cryostats)	2
Shape	Rectangular
Drift cell configuration within module	3 wide × 2 high × 18 long drift cells
Drift cell dimensions	2 × 3.7 m wide (drift) × 7 m high × 2.5 m long
Detector module dimensions	22.4 m wide × 14 m high × 45.6 m long
Anode wire spacing	~5 mm
Wire planes (orientation from vertical)	Grid (0°), Induction 1 (45°), Induction 2 (−45°), and Collection (0°)
Scintillation light detection	Yes
Photon yield	>1 pe /10 MeV
Drift electric field	500 V/cm
Maximum drift time	2.3 ms
Signal/noise for 1 MIP	~9

beamline-measurements system (BLM) and a neutrino-detection system (ND for "neutrino detectors"). The near detectors will be located at the near site (Fermilab), downstream of the beamline. The BLM will be located in the region of the Absorber Complex at the downstream end of the decay region to measure the muon fluxes from hadron decay. The neutrino detector will be placed in the near detector hall, 450 m downstream of the target, and underground. The reference-design neutrino measurements system technology is a liquid-argon-filled time projection chamber tracker (LArTPCT), matching the interaction material in the LAr-FD (described in Volume 4 of this CDR). The LArTPCT will consist of a 1.8 m × 6 m × 1.8 m × 4 m TPC and a 2.7 m diameter × 5 m long LAr cryostat inside of a large dipole magnet. This system is intended to measure the various neutrino fluxes and spectra and to measure the neutrino interaction channels important for predicting the signals and backgrounds at the far site.

2.2. Scientific Sensitivity. The LBNE project has a broad range of scientific objectives, listed below.

(1) Measurements of the parameters that govern $\nu_\mu \rightarrow \nu_e$ oscillations as discussed above. These include measurement of the CP violating phase δ_{CP} and determination of the mass ordering (the sign of Δm^2_{32}).

(2) Precision measurements of θ_{23} and $-\Delta m^2_{32}-$ in the ν_μ-disappearance channel.

(3) Search for proton decay, yielding measurement of the partial lifetime of the proton (τ/BR) in one or more important candidate decay modes, for example, $p \rightarrow e^+\pi^0$ or $p \rightarrow K^+\nu$, or significant improvement in limits on it.

(4) Detection and measurement of the neutrino flux from a core-collapse supernova within our galaxy or a nearby galaxy, should one occur during the lifetime of the detector.

(5) Other accelerator-based neutrino oscillation measurements.

(6) Measurements of neutrino oscillation phenomena using atmospheric neutrinos.

(7) Measurement of other astrophysical phenomena using medium-energy neutrinos.

The detector design was driven largely by objectives (1)–(4).

Observation of $\nu_\mu \rightarrow \nu_e$ oscillations will allow us to determine the neutrino mass hierarchy and measure leptonic CP violation through the measurement of δ_{CP}. In five years of neutrino (antineutrino) running, assuming $\sin^2(2\theta_{13}) \sim 0.1$, $\delta_{CP} = 0$, and normal mass hierarchy, we expect 1160 (330) selected ν_e or $\overline{\nu}_e$ signal events with 300 (180) background events in a 34 kt liquid argon TPC detector with a 700 kW beam.

Figure 6 shows the fraction of possible δ_{CP} values covered at the 3σ level for determining $\sin^2(2\theta_{13}) \neq 0$, the mass hierarchy, and CP violation as a function of $\sin^2(2\theta_{13})$ for a 34 kt detector in a 700 kW beam running for five years in neutrino mode and five years in antineutrino mode. At a value of $\sin^2(2\theta_{13}) = 0.1$ (the measured value from Daya Bay), the mass hierarchy can be resolved at $>3\sigma$ for 100% of δ_{CP}. For CP violation, a 3σ determination can be made for ~65% of δ_{CP} values.

In addition, a liquid argon detector of this size can achieve <1% precision on measurements of Δm^2_{32} and $\sin^2(2\theta_{23})$ through muon neutrino and antineutrino disappearance. There is also the potential to resolve the θ_{23} octant degeneracy and improve model-independent bounds on nonstandard interactions.

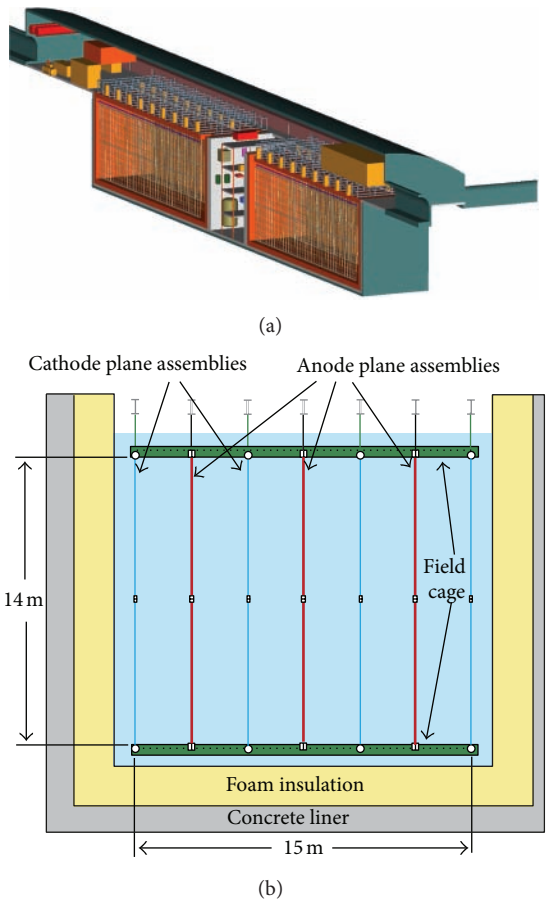

Figure 5: Detector configuration within the cavern. The TPC is located within a membrane cryostat, shown in orange. The interior dimensions of each cryostat are 24 m wide × 18 m high × 51 m long. The highbay is 150 m long and has a 32 m span. Cryogenic equipment is located in the septum area between the two cryostats. The right-hand side shows a cut view of the cryostat. The anode and cathode wire planes are hung from the ceiling of the cryostat. Each anode plane consists of u/v readout wires wrapped around a stainless steel frame and readout by electronics mounted on the planes.

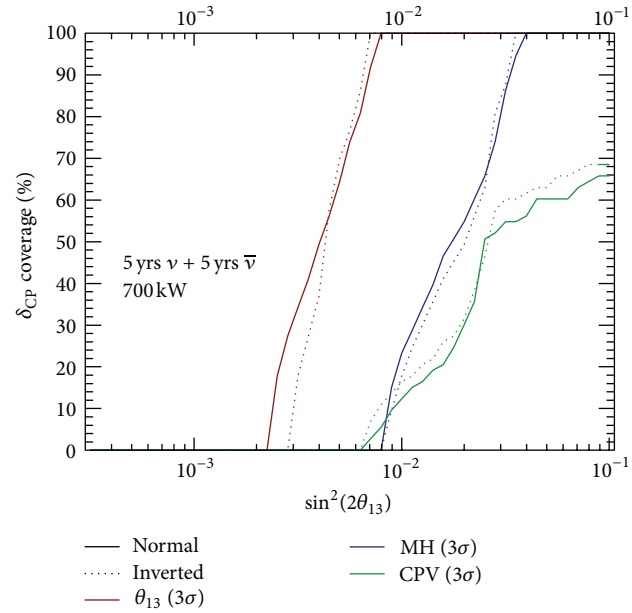

Figure 6: 3σ discovery potential for determining $\sin^2(2\theta_{13}) \neq 0$ (red), the mass hierarchy (blue), and CP violation (green) as a function of $\sin^2(2\theta_{13})$ and the fraction of δ_{CP} coverage. The sensitivities are shown for both normal (solid) and inverted (dashed) mass hierarchies for a 34 kt LAr detector given five years running in ν mode + five years in $\overline{\nu}$ mode in a 700 kW beam.

The scientific capability for detection of nucleon decay and supernova using a large liquid argon TPC has been discussed elsewhere in this paper. We will not cover it in detail here. The 34 kt liquid argon TPC can achieve sensitivity to proton lifetimes of ~5×10^{34} years after 10 yrs of running at 90% CL. If the detector energy threshold of ~10 MeV can be achieved, then a galactic supernova burst at 10 kpc will produce over 3000 events. The threshold of the LArTPC depends on the data rate due to either the electronic noise or the background due to radioactivity in the detector either because of activity from the materials or because of spallation products due to cosmic ray muons. In case of a burst of supernova neutrino events, the photon system can be used to identify the burst rapidly, but each individual event is measured by the TPC. The LBNE cold electronics design keeps the electronic noise level at a low level so that a 10 MeV threshold can be easily achieved; however, the minimum depth requirement for spallation backgrounds is still under investigation. The liquid argon detector will also have unique and high-precision capability with respect to atmospheric neutrinos. The key detector requirement for nonaccelerator physics is the depth of the detector. The design depth of 4850 ft for the LBNE far detector has been evaluated to be sufficient for nonaccelerator physics [20].

2.3. Phases or Alternatives for LBNE. The cost of the LBNE project includes the design and constructions of the beamline, the far and near detectors, and the surface and underground civil constructions needed for the beamline and to house the detectors and shield them from cosmic rays. A preliminary cost and schedule estimate for the entire project was assembled and reviewed in March 2012. The costs include the engineering and scientific manpower that is needed for the design and construction activities. It also includes appropriate contingencies and overheads. The total cost for the project as described above is approximately US $1.5 B in FY2010 currency. The schedule for the project partly depends on the availability of funds; however a preliminary technical evaluation of the schedule suggests an experiment start in year ~2022.

The cost of the complete LBNE project is considered too high for the current budgetary climate in the US, and, therefore, the US, Department of Energy has asked for an approach to reach the scientific goals of LBNE in a phased manner. Furthermore, strategies and consultation are sought to enhance international participation in the project. In response to this request, various phasing strategies as well as alternatives have been examined. To address all of the

fundamental science goals listed above, a reconfigured LBNE would need a very long baseline (>1,000 km from accelerator to detector) and a large detector deep underground. However, it is not possible to meet all of these requirements in a first phase of the experiment within the budget guideline of about half of the projected cost of the full project.

Therefore, options are being assessed that meet some of the requirements, and three viable options have been identified for a Phase 1 long-baseline experiment that have the potential to accomplish important science at realizable cost. There are listed below.

(i) Using the existing NuMI beamline in the low-energy configuration with a 30 kt liquid argon time projection chamber (LAr-TPC) surface detector 14 mrad off-axis at Ash River in Minnesota, 810 km from Fermilab.

(ii) Using the existing NuMI beamline in the low-energy configuration with a 15 kt LAr-TPC underground (at the 2340 ft level) detector on-axis at the Soudan mine in Minnesota near the MINOS detector, 735 km from Fermilab.

(iii) Constructing a new low-energy LBNE beamline with a 10 kt LAr-TPC surface detector on-axis at Homestake in South Dakota, 1,300 km from Fermilab.

The scientific capabilities of the above options have been discussed in [21]. While each of these first-phase options is stronger than the others in some particular domain, the option to build a new beamline to Homestake with an initial 10 kt LAr-TPC detector on or near the surface is strongly favored. The neutrino beam physics reach of this first phase is comprehensive with good sensitivity to all important parameters.

This option is seen as a start of a long-term program that would achieve the full goals of LBNE in time and allow probing the standard model most incisively beyond its current state. Ultimately this option would exploit the full power provided by Project-X. At the present level of cost estimation, it appears that this preferred option may be 10% more expensive than the other two options, but cost evaluations are continuing. The major limitation of the preferred option is that the underground physics program including proton decay and supernova collapse cannot start until later phases of the project. Placing a 10 kt detector underground instead of the surface in the first phase would allow such a start and increase the cost by about $135 M. Negotiations to obtain such funding from US domestic funding sources or international participants are in progress.

2.4. High-Intensity Accelerator Upgrades in the US. Project-X is a multimegawatt proton facility being developed to support intensity frontier research in elementary particle physics, with possible applications to nuclear physics and nuclear energy research, at Fermilab. The centerpiece of this program is a superconducting H^- linac that will support programs in long-baseline neutrino experiments and the study of rare kaon and muon processes. Based on technology shared with the International Linear Collider (ILC), Project-X will provide multi-MW beams at 60–120 GeV from the Main Injector, simultaneous with very-high-intensity beams at lower energies. Details of Project-X design can be obtained from [18].

In Table 3, we have made a list of beam conditions that could be possible from Project-X and further Project-X upgrade at 8 GeV. Figure 7 shows the beam power available from the Main Injector as a function of energy. With Project-X the beam power from the Main Injector can be maintained at or above 2 MW over the range 60–120 GeV. This is because the decrease in energy can be (mostly) compensated by increasing the repetition rate. This trend continues as the energy decreases, but at some point it is limited by the number of protons coming from the linac. The power achievable at 30 GeV would be ~1.3 MW for the Project-X reference design. The Main Injector requires 270 kW of incident 8 GeV beam power at 8 GeV to produce ~2 MW at 60 GeV. With additional upgrades to the 8 GeV pulsed linac, the 8 GeV power level could be increased to ~4 MW. In such a scenario, the Fermilab accelerator complex could produce multi-MW power at both 60 GeV and 8 GeV simultaneously. The duty factor for any Main Injector operation would continue to remain small in the single turn extraction mode; however, the duty factor at 8 GeV will be ~5–10% unless a ring is deployed to compress the beam further. The large-intensity increase from these accelerator upgrades at FNAL would greatly improve the precision of long-baseline neutrino science. The event spectra and experimental approaches using possible beams from high-intensity protons are in [22]. The precision on the parameters $\sin^2 2\theta_{13}$ and δ_{CP} is shown in Figure 8 using the full simulation of the LBNE beam and the expected performance of a 34 kt liquid argon TPC detector [23]. The calculation of the sensitivity was performed using the GLOBeS software tool which allows careful consideration of all parameter correlations and ambiguities. The long baseline and broadband beam for LBNE allows for determination of the parameters with no remaining ambiguities.

3. The Japanese Approach

Based on the indication of $\nu_\mu \rightarrow \nu_e$ conversion phenomenon demonstrated by T2K [25] and subsequent confirmation by reactor experiments [26–28], a next-generation experiment aimed at the discovery of CP violation in the lepton sector would be recommended with high priority.

In Japan, two different approaches are considered for the study of lepton CP symmetry using the neutrino beam at J-PARC. One configuration is suitable for water Cherenkov technology, and the other is suitable for liquid argon TPC technology. Since water Cherenkov technology has an excellent performance for a sub-GeV low multiplicity final state environment, a relatively short baseline of 295 km with a low-energy narrowband neutrino beam is adopted to compare the difference between ν_e and $\overline{\nu}_e$ charged current events from appearance results at the first neutrino oscillation maximum. In the case of a Liquid argon TPC, since this technology has an excellent energy resolution for neutrino

Table 3: Beam conditions and power possible during the Project-X phase and further upgrades to the 8 GeV performance. An accumulator ring at 8 GeV could be used to improve the duty factor.

Accelerator stage	Energy	Current	Duty factor	Power available
Continuous wave linac	3 GeV	1 mA	Continuous wave	3000 kW
Pulsed linac	8 GeV	43 μA	4.33 ms/0.1 sec	350 kW
8 GeV upgrade	8 GeV	500 μA	6.67 ms/0.066 sec	4000 kW
Main injector	60 GeV	35 μA	9.5 μS/0.7 sec	2100 kW
Main injector	120 GeV	19 μA	9.5 μS/1.3 sec	2300 kW

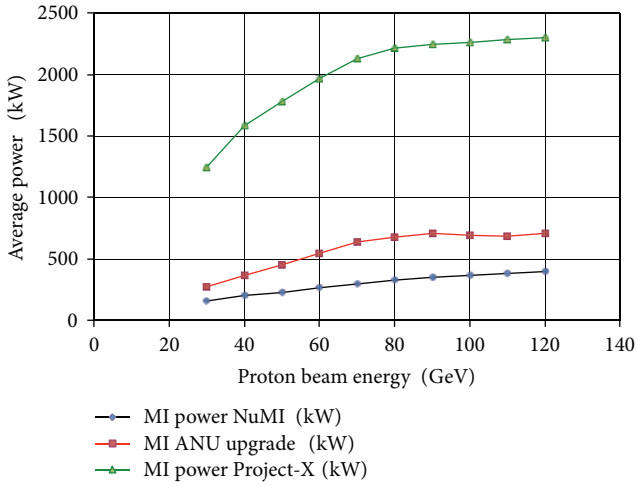

Figure 7: Proton beam power as a function of proton energy from the Fermilab Main Injector. Shown are current capabilities labeled as NuMI. The recently funded upgrades (labeled as ANU) will increase the power to 550 kW at 60 GeV or 700 kW at 120 GeV. Project-X as currently conceived will allow beam power of 2 MW at 60 GeV and 2.3 MW at 120 GeV.

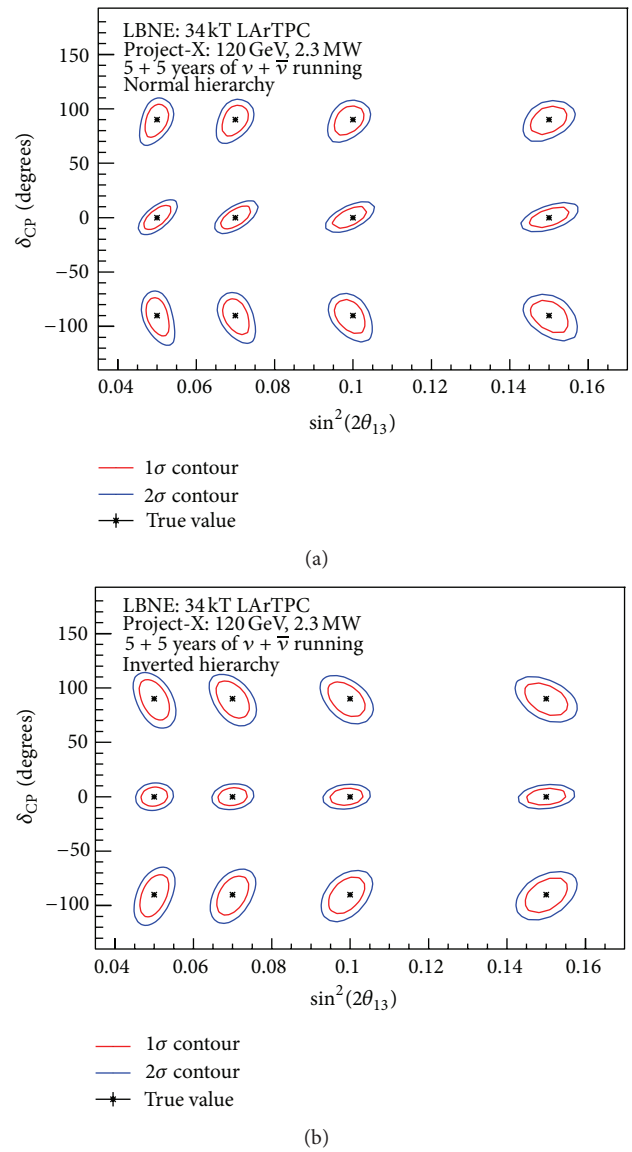

Figure 8: Precision on parameters $\sin^2 2\theta_{13}$ and δ_{CP} from the LBNE configuration using high-intensity beam from Project-X. The precision is shown as for various true parameters across the δ_{CP} and $\sin^2 2\theta_{13}$ space. This calculation was performed with the GLOBeS sensitivity calculation tool [24] which marginalizes over all oscillation parameters, except for the ones being fit, including the mass hierarchy using known errors. The long-baseline LBNE setup allows separation of matter and CP effects with no remaining ambiguities because of the length of the baseline and the broadband beam.

energy measurement and an event reconstruction capability for a wide energy range, a relatively long baseline of 658 km with a wideband neutrino beam is adopted to precisely measure the ν_e and $\overline{\nu}_e$ appearance energy spectrum shape (peak position and height for 1st and 2nd neutrino oscillation maximum and minimum). Given the assumed location of each detector, namely, a 560 kt water Cherenkov detector (hyper-Kamiokande) at Kamioka, and a 100 kt liquid Argon TPC at Okinoshima, the required beam conditions for both approaches are satisfactorily provided by the single J-PARC neutrino beam simultaneously.

In this section we describe the Japanese approach, including the accelerator-based neutrino source in Japan, the Okinoshima Giant Liquid Argon Observatory, and the Hyper-Kamiokande project.

3.1. Accelerator-Based Neutrino Source in Japan

3.1.1. J-PARC and the Main Ring Synchrotron. J-PARC (Japan Proton Accelerator Research Complex) is a KEK-JAEA joint facility of a MW-class high-intensity proton accelerator research facility (Figure 9) [29]. It provides an unprecedented high flux of various secondary particles, such as neutrons,

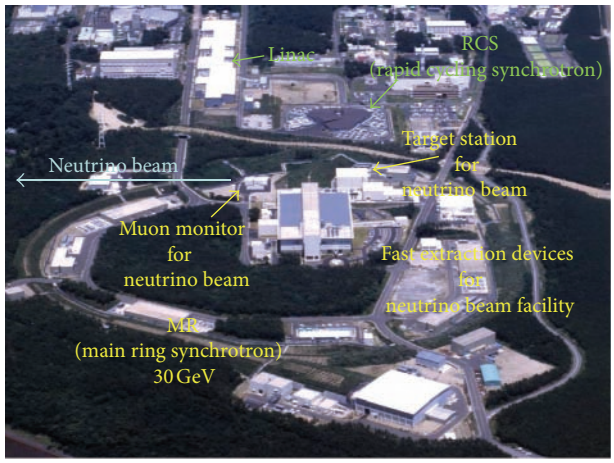

Figure 9: J-PARC accelerator and experimental facility.

muons, pions, kaons, and neutrinos, which are utilized for elementary particle physics and material and life science.

In the accelerator complex, H^- ions are accelerated to 181 MeV with a linac, fed into the rapid cycling synchrotron (RCS) with electrons stripped, and then accelerated to 3 GeV. At the final stage, the proton beam goes into main ring synchrotron and is accelerated to 30 GeV. For the neutrino experiment, accelerated protons are kicked inward to the neutrino beam facility in a single turn with fast extraction devices.

3.1.2. The J-PARC Neutrino Beam Facility. The proton beam from the main ring synchrotron (MR) travels the J-PARC neutrino beam facility and produces an intense beam of muon neutrinos pointing west. The J-PARC neutrino beam facility is composed of the following components (Figure 10) [29].

(i) Preparation section: matches the beam optics to the arc section.

(ii) Arc section: bends the beam ~90° toward the west direction with a superconducting combined function magnet.

(iii) Final focus section: matches the beam optics to the target both in position and in profile. The level of control at the mm level is necessary which corresponds to 1 mrad ν direction difference. It is also important in order not to destroy the target.

(iv) Graphite target and horn magnet: produce intense secondary π's and focus them toward the west. There are 3 horns with 250 kA pulse operation.

(v) Muon monitor: monitors the μ direction (= ν direction) pulse to pulse by measuring the centre of the muon profile.

(vi) On-axis neutrino monitor: monitors the ν direction and intensity.

This facility is designed to be tolerate around ~1 MW beam power. This limitation is due to the temperature rise and thermal shock for the components such as the Al horn, graphite target, and Ti vacuum window. Since this region is a high-radiation environment, a careful treatment of the radioactive water and air is required. Moreover, a maintenance scenario of radioactive components has to be carefully planned.

3.1.3. J-PARC Neutrino Beam Intensity Upgrade Plan. Till June 2012 the J-PARC neutrino beam delivered up to 0.19 MW to T2K (Tokai-to-Kamioka long-baseline neutrino experiment) [29]. With the goal of the improvement of the neutrino beam intensity, an MR power improvement scenario has been analyzed. The proposal by the J-PARC accelerator team is shown in Table 4.

The items to be modified are listed as follows.

(i) For the linac, a 400 MeV operation is required to avoid severe space charge effects at RCS injection. The installation of necessary equipment is foreseen from the summer of 2013.

(ii) The repetition cycle of the MR has to be improved from 2.56 seconds to 1.28 seconds. For this purpose, the RF and the magnet power supply improvements are necessary. The necessary R&D for these components has been started as of 2012.

(iii) A system to localize the beam loss at the dedicated collimator system must be installed.

Assuming a successful R&D program on the higher repetition cycle and on the increase of the number of particles per bunch as well as sufficient resources the accelerator power will be upgraded to 0.75 MW within a time scale of five years.

3.2. The Okinoshima Giant Liquid Argon Observatory. The use of a giant liquid argon time projection chamber (TPC) with 100 kton size is an excellent opportunity to realize a broad range of scientific topics. It would be ideal for the next-generation accelerator-based neutrino research investigating the lepton sector CP symmetry and would extend the search for the proton decay via modes favored by the supersymmetric grand unified models (e.g., $p \rightarrow \nu K^+$) up to 10^{35} years. Moreover, it would cover a wide range of neutrino physics stemming from astrophysical and terrestrial sources (e.g., solar and atmospheric neutrinos, neutrinos from stellar collapse and the neutrinos from dark matter annihilation). Specifications of the assumed detector are described in Table 5.

3.2.1. Optimal Configuration for the Investigation of Lepton Sector CP Phase δ_{CP} with a Liquid Argon TPC . The effects of lepton sector CP phase δ_{CP} appear either

(1) in the energy spectrum shape of the appearance oscillated ν_e charged current events (sensitive to all the nonvanishing δ_{CP} values including 180°) or

(2) as a difference between ν and $\bar{\nu}$ behaviors (this is sensitive to the CP-odd term which vanishes for δ_{CP} = 0 or 180°).

Table 4: MR power improvement scenario.

	Till June 2012	Next step	Target
Power (MW)	0.19	0.30	**0.75**
Energy (GeV)	30	30	**30**
Rep. cycle (sec.)	2.56	2.40	**1.28**
No. of bunches	8	8	**8**
Particles/bunch	1.26×10^{13}	1.9×10^{13}	$\mathbf{2.5 \times 10^{13}}$
Particles/ring	1.0×10^{14}	1.5×10^{14}	$\mathbf{2.0 \times 10^{14}}$
Linac (MeV)	181	400	**400**
RCS[a]	$h = 2$	$h = 2$	$\mathbf{h = 2}$

[a]Harmonic member of RCS.

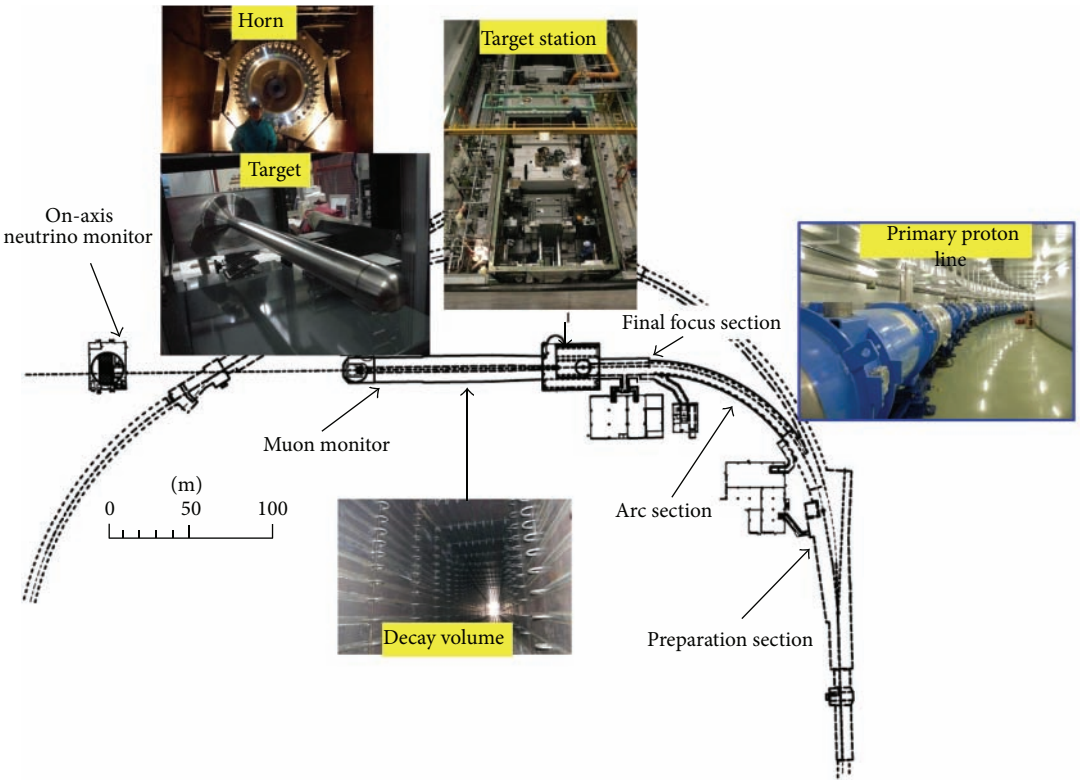

Figure 10: J-PARC neutrino beam facility.

It should be noted that if one precisely measures the ν_e appearance energy spectrum shape (peak position and height for 1st and 2nd oscillation maximum and minimum) with high resolution, the CP effect could be investigated with neutrino running only. On the other hand, if one tries to extract CP information by comparing ν and $\overline{\nu}$ behaviour, it is necessary to run in antineutrino mode as well. Antineutrino beam conditions are known to be more difficult than those for neutrinos due to the lower beam flux, the leading charge effect in proton collisions on target, smaller antineutrino cross-sections at low energy, and so forth. Moreover, the systematic uncertainties for the neutrino mode experiment and antineutrino mode experiment are different and not much cancellation is foreseen.

An optimal experimental setup including parameters such as the length of the baseline, the angle with respect to the neutrino beam axis and the detector technology affects the extraction of the CP phase [30]. Since the liquid argon TPC has an excellent energy resolution for the neutrino energy measurement and event reconstruction capability from sub-GeV to a few GeV and from single prong to high multiplicity configurations, it is suitable for spectrum measurement with wide energy coverage. To precisely measure the ν_e and $\overline{\nu}_e$ appearance energy, spectrum shape an on-axis wide band beam is necessary. In order to enable the measurement of the 2nd neutrino oscillation maximum, the energy of the 2nd neutrino oscillation maximum has to be set above about 400 MeV. As a consequence, the position of the 1st neutrino oscillation maximum, which also has to be measured, is also at a higher energy. As a consequence, events associated with $\pi^0 s$ originating from high-energy neutrino interactions will have to be dealt with as these mimic the signal ν_e ($\overline{\nu}_e$) charged current interaction. Therefore, a good discrimination between $\pi^0 s$ and electrons is indispensable for the required

Table 5: Specification of giant liquid argon time projection chamber.

Diameter for active argon (m)	70
Drift length (m)	20
Active mass (ton)	107753
Signal readout area (m^2)	3848
Maximum drift time at 1 kV/cm (ms)	10
Charge readout views	3 mm pitch, two perpendicular strips
Scintillation light readout	1000 8″ PMT

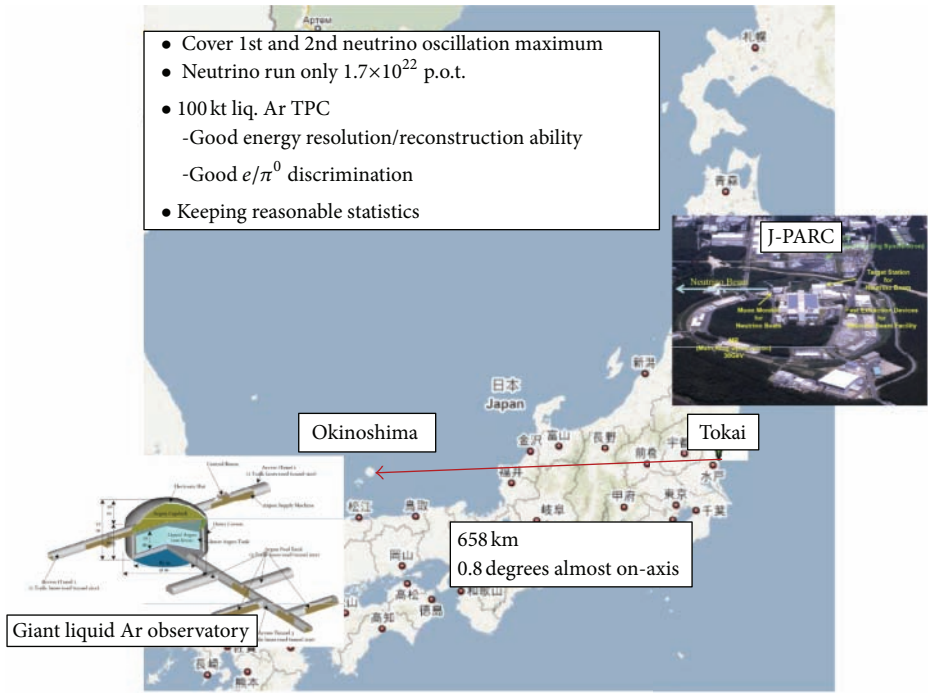

Figure 11: J-PARC to Okinoshima long-baseline neutrino experiment.

experimental configuration. Since the liquid argon TPC has an excellent discrimination capability between $\pi^0 s$ and electrons, a wideband on-axis beam for spectrum measurement is desirable.

In order to realize the project within a reasonable time scale, it makes sense to utilize the currently available facilities as much as possible. On the other hand, this may present boundary conditions for the project. In our case, J-PARC is a currently available and indispensable facility for our project. We have to consider the project taking into account its available intensity (750 kW) and energy (30 GeV). To obtain an experimental result within a reasonable time scale, it would be preferable if we could extract lepton CP symmetry information without relying on a time-consuming antineutrino beam setting. If the baseline of the experiment becomes longer, the neutrino energy has to increase in order to fit the neutrino spectrum within the neutrino oscillation maximum. Given the proton accelerator energy setting, which creates a limitation on the available neutrino energy, there is a limitation on the baseline of the experiment, accordingly.

Thus, the optimal choice for the investigation of lepton sector CP symmetry using a liquid argon TPC is the measurement of the energy spectrum shape of the appearance oscillated ν_e charged current events (with an emphasis on the 1st and 2nd oscillation maximum) using an on-axis neutrino beam. After this first phase measurement, an antineutrino beam (opposite horn polarity) experiment might be considered in a second stage in order to crosscheck the results obtained with the neutrino run.

The necessary conditions for the measurement are

(1) a long baseline (>600 km) to see the second oscillation maximum in a measurable energy region (>400 MeV),

(2) an on-axis beam for wide energy coverage, and

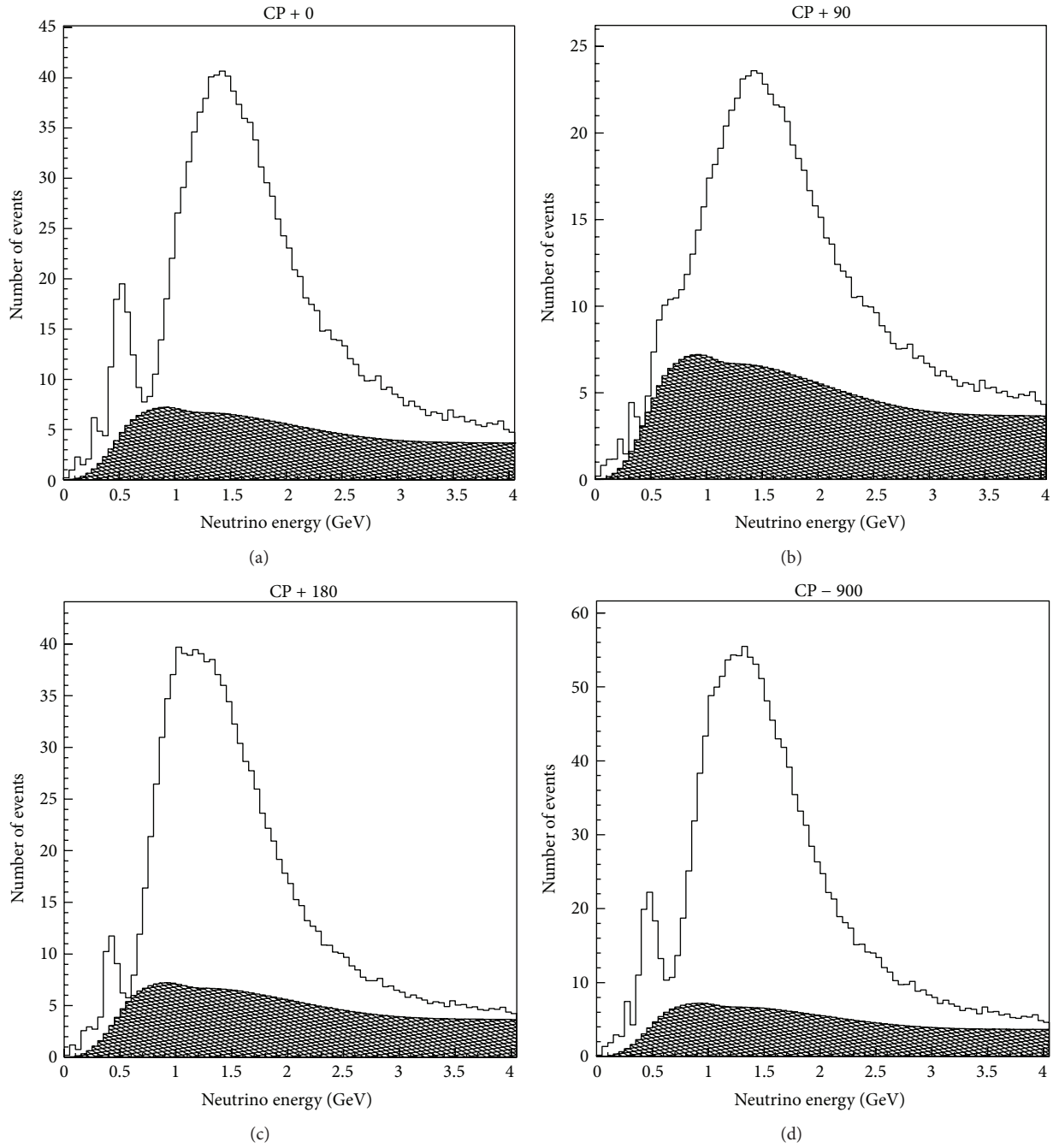

FIGURE 12: Energy spectra at $\sin^2 2\theta_{13} = 0.03$ and normal mass hierarchy case, with $\delta_{CP} = 0^\circ$ (a), 90° (b), 180°(c), and 270° (d) cases.

(3) a giant detector to overcome the finite beam flux and long baseline.

3.2.2. The J-PARC to Okinoshima Long-Baseline Neutrino Experiment with 100 kton Liquid Argon TPC. With the same configuration as T2K (2.5° off-axis angle), the center of the neutrino beam will traverse the earth and reach Okinoshima island (658 km baseline) with an off-axis angle 0.76° (almost on-axis). The scenario is depicted in Figure 11 [1].

The analysis presented here is based on the assumption of a neutrino run only with an exposure of 1.7×10^{22} protons on a pion production target. The detector is assumed to be a 100 kton liquid argon TPC. This type of detector should provide higher precision than other huge detectors to separate the two peaks in the energy spectrum. In addition, since the π^0 background is expected to be highly suppressed due to the fine granularity of the readout, the main irreducible background will be the intrinsic ν_e component of the beam.

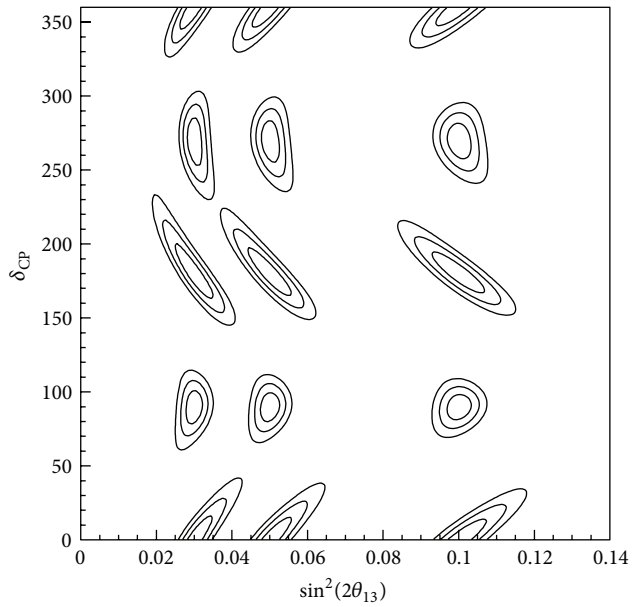

Figure 13: Allowed regions in the perfect resolution case. Twelve allowed regions are overlaid for twelve true values, $\sin^2 2\theta_{13} = 0.1$, 0.05, 0.02, and $\delta_{CP} = 0^\circ, 90^\circ, 180^\circ, 270^\circ$. The outermost boundary of the circles correspond to 3σ.

Figure 12 shows the energy spectra of electron neutrinos for the cases of δ_{CP} equal 0°, 90°, 180°, and 270° with normal mass hierarchy. The shaded region is common for all plots and shows the background from intrinsic beam ν_e. Simulation includes smearing due to Fermi motion of nucleons in Argon nuclei. Here, a perfect resolution for the energy measurement of neutrinos is assumed. According to the simulation study, an energy measurement resolution of about 10% R.M.S. is expected. As shown, the value of δ_{CP} affects the energy spectrum, especially in the first and the second oscillation peaks (heights and positions). Therefore, a comparison of the peaks can determine the value δ_{CP}, while the value of $\sin^2 2\theta_{13}$ changes the number of events predominantly.

Allowed regions in the perfect resolution case are shown in Figure 13. Twelve allowed regions are overlaid for twelve true values, $\sin^2 2\theta_{13} = 0.1$, 0.05, 0.02, and $\delta_{CP} = 0^\circ, 90^\circ, 180^\circ, 270^\circ$, respectively. The 3σ sensitivity for the δ_{CP} is 20–30° depending on the true δ_{CP} value [1].

3.2.3. Okinoshima Site Study. The site study of the Okinoshima Giant Liquid Argon Observatory has been initiated taking into account geological, geographical, and infrastructure considerations [32].

The main island of Okinoshima, Dogo, is almost circular with a diameter of about 16 km and the center is a mountainous zone with an altitude of 500 m and more than one candidate location for the giant liquid argon observatory can be found. The distance from the main island of Japan (Honshu) is about 80 km. The population is about 16,000 and the economy mainly depends on the fishery and tourist business.

Though the islands were born of volcanic activity around 5 to 6 million years ago, there is stable bedrock, called Oki-Gneiss, which is the oldest rock in Japan (more than 3 billion years old) and which is suitable for the construction of a big cavern. Typical specific gravity and axial strength of Oki-Gneiss is 27 kN/m^3 and 79 MPa, respectively.

The cross-sectional drawing of the potential location of the cavern is shown in Figure 14. Since a shallow depth (>600 m water equivalent) is enough to suppress cosmogenic background for a liquid argon TPC [33], horizontal access from the outside is assumed. The earth covering between the top of the cavern and the mountain top is 252 m. Simulation study indicates that there are 1 to 2 muons/10 msec in the assumed 100 kt liquid Ar TPC configuration (10 msec corresponds to the signal electron drift time for an assumed 20 m drift distance.). Therefore, it is judged that the number of muons is small enough to operate the detector. If necessary, the bottom of the cavern could be lowered, for instance, by another 100 m.

A conceptual design of the cavern has been carried out and is also shown in Figure 14. In order to contain a cylindrical 100 kton liquid argon observatory with a base diameter of 80 m and a height of 20 m, the inner dimensions of the cylindrical cavern should provide a base diameter of 91 m, a height of 20 m, and a spherical cap of 20 m in height.

There would not be a difficulty in transportation since there are regular daily commercial connecting flights and ferry services between Honshu and the main harbor of Dogo (Saigou port) which is close to the location of the candidate site. Moreover, there is a sufficient traffic access route between Saigou port and the candidate site to carry heavy equipment needed for the civil engineering work, the large amount of liquid argon, and the detector components.

The Chugoku Electric Power Company provides electricity for Okinoshima. The existing total electricity capacity is 32 MW and may be enough for the construction and operation of the observatory.

The procurement of 100 kton of liquid argon, which should be done within about 5 years with minimum cost, is another important issue to be considered. One possible solution is to

(1) purchase liquid Argon from several large-scale manufacturing plants which have large production capacities. The demand from the Giant Liquid Argon Observatory is estimated to be roughly 10 to 15% of their annual production capacity;

(2) hire 4 tanker trucks dedicated for the liquid Argon ground transportation. The cost of trucks for 5 years is not the major part of the total cost for the project.

So far there is no show stopper to realize the Okinoshima Giant Liquid Argon Observatory.

3.3. The Hyper-Kamiokande Project. Hyper-Kamiokande (Hyper-K), being proposed by the Hyper-Kamiokande working group [2], is the third-generation underground water Cherenkov detector at Kamioka that serves as a far detector of a long-baseline neutrino oscillation experiment

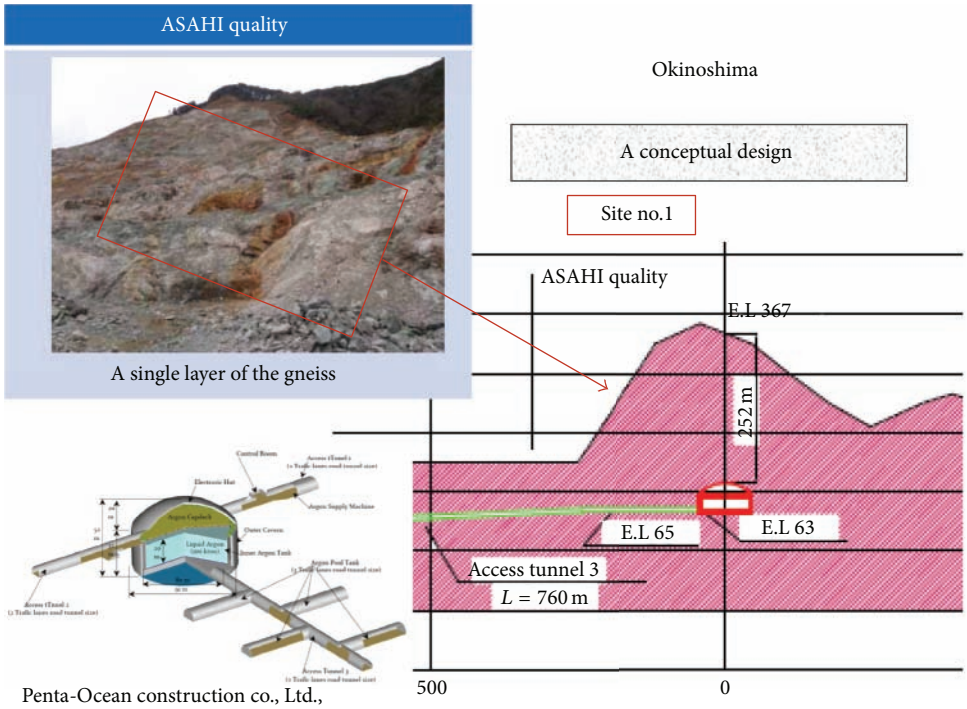

Figure 14: Potential cavern for Okinoshima Giant Liquid Argon Observatory.

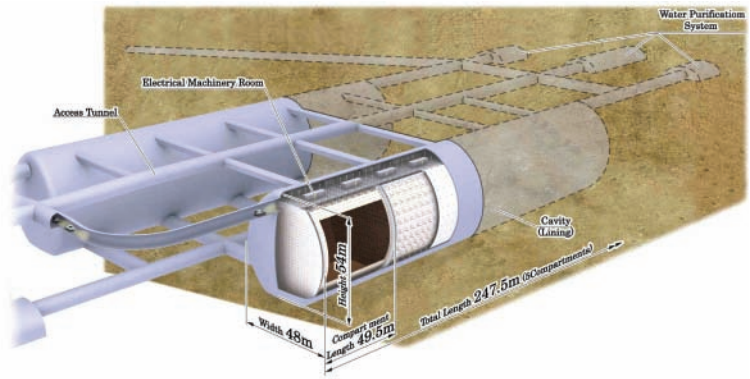

Figure 15: Schematic view of the Hyper-Kamiokande detector. The detector consists of two cylindrical water tanks lying side by side.

for the J-PARC neutrino beam and as a detector capable of observing proton decays, atmospheric neutrinos, and neutrinos from other astrophysical origins. The baseline design of the Hyper-K project is determined based on the established water Cherenkov detector technology in the successful Super-Kamiokande (Super-K) experiment. Its physics potential is estimated based on the detector performance proven by the Super-K detector.

The schematic view of the Hyper-K is shown in Figure 15. Table 6 summarizes the baseline design parameters of the Hyper-K detector. The detector consists of two cylindrical water tanks lying side by side. The water tank has dimensions of 54 (H) × 48 (W) × 250 (L) m^3, containing 0.5 × 2 ~ 0.99 million metric tonnes (mton) of ultra pure water in total. The fiducial volume of the two tanks is 0.56 mton and is 25 times larger than the fiducial volume of Super-K. The detector will be optically separated into ten subdetectors by 50 m spacing segmentation walls and each subdetector is viewed by photomultiplier tubes (PMTs) to detect Cherenkov photons emitted by charged particles traversing the tank water. In the baseline design, 99,000 20 inch HAMAMATSU R3600 PMTs will be implemented on the detector walls to achieve 20% photocoverage, about half that of Super-K. The 2 m thick outer detector layers completely surround the inner detector volume and are instrumented with 8 inch PMTs.

The Hyper-K detector candidate site, located 8 km south of the Super-K, is in the Tochibora mine of the Kamioka Mining and Smelting Company, near Kamioka town in Gifu prefecture, Japan. The experiment site is accessible via a drive-in, 2.6 km long, horizontal mine tunnel. The detector will lie under the peak of Nijuugo-yama, having 648 meters of rock or 1,750 meters-water-equivalent (m.w.e.) overburden.

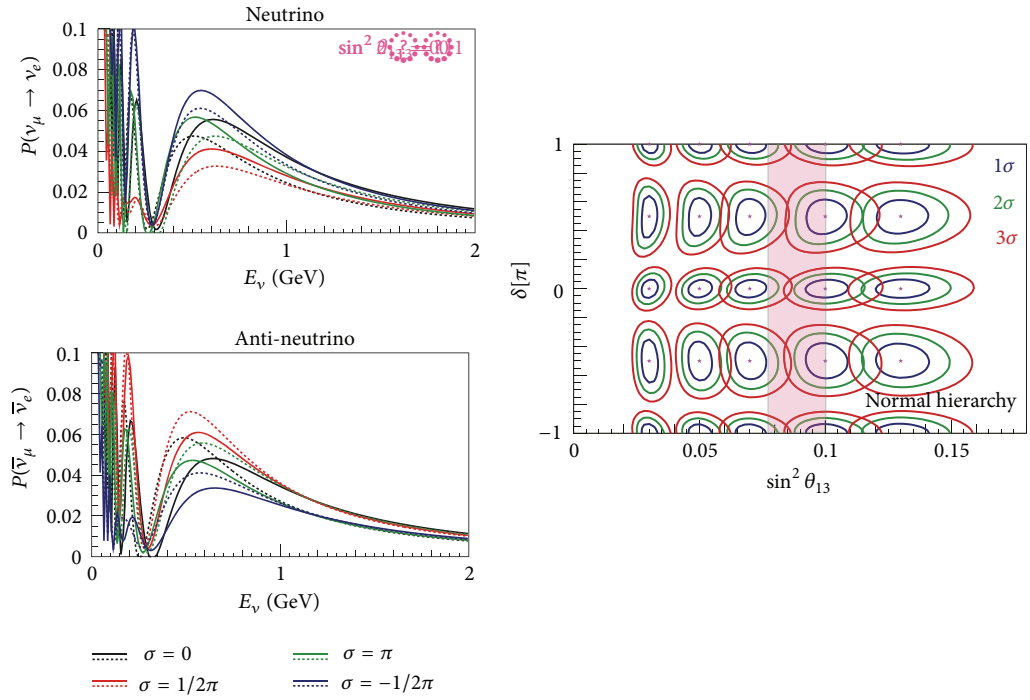

FIGURE 16: Transition probability of muon neutrino to electron neutrino at the distance of 295 km for neutrino (left top panel) and antineutrino (right top). Each color shows the appearance probability for each δ_{CP} values. Solid and dashed lines represent normal and inverted mass hierarchy, respectively. The right panel shows expected contours for each true $(\delta, \sin^2 2\theta_{13})$ parameter set by 7.5 MW·years JPARC-HK long-baseline neutrino oscillation experiment. Three colors show 1, 2, and 3 σ significance. The pink band corresponds to the θ_{13} value measured by the Daya Bay reactor experiment [31].

The cosmic ray muon rate at the candidate site is reduced to $1.0 - 2.3 \times 10^{-6}$ s^{-1} cm^{-2} which enables us to perform nonaccelerator physics research programs. The off-axis angle for the J-PARC neutrino beam is 2.5° and the baseline is 295 km, both are same as those of the Super-K in the ongoing T2K experiment.

The expected detector performance of Hyper-K, assuming 20% photocoverage, is summarized in Table 7. The efficiency of ν_e appearance signal for the J-PARC neutrino beam is as high as ~60% while keeping excellent background rejection efficiency of 99.9% for $\nu_\mu + \bar{\nu}_\mu$ CC and 95% for NC π^0 interactions. We may improve the rejection efficiency in the future to optimize the leptonic CP violation search.

Hyper-K provides rich neutrino physics programs as summarized in Table 8. In particular, it will provide unprecedented discovery potential of leptonic CP violation by comparing $\nu_\mu \to \nu_e$ and $\bar{\nu}_\mu \to \bar{\nu}_e$ probabilities in J-PARC neutrino beam as shown in the left two panels of Figure 16. The right panel in Figure 16 shows an expected size of contours for each true $(\delta, \sin^2 2\theta_{13})$ parameter set. By using 3.75 MW·years of J-PARC neutrino beam, where 1 year is equivalent to 10^7 seconds and the run time ratio of neutrino mode and antineutrino mode is assumed to be 1.5 : 3.5, Hyper-K will provide 3σ discovery reaching the leptonic CP violation for 69% of the δ parameter space if the mass hierarchy is known. The accuracy of δ determination is better than 20° at 1σ and does not depend much on true θ_{13} value. If the beam time is increased to 7.5 MW·years, the discovery coverage extends to 74% of the δ parameter space. If the mass hierarchy is unknown, the sensitivity to the CP violation is somewhat reduced due to degeneracy. However, the mass hierarchy can be determined with more than 3σ significance for 43% (44%) of the δ parameter space for normal (inverted) mass hierarchy if $\sin^2 2\theta_{13} = 0.1$ as measured by the reactor neutrino oscillation experiments.

Natural, free, and atmospheric neutrinos also provide a good opportunity to study neutrino properties. In particular, thanks to the relatively large $\sin^2 2\theta_{13}$ value of ~0.1, there is a good chance to determine the neutrino mass hierarchy by testing the ν_e (or $\bar{\nu}_e$) enhancements via MSW resonance effect by Earth's matter. As illustrated in Figure 17, the ν_e flux enhancement happens in 5–10 GeV upward going neutrinos in the case that the mass ordering is normal. In the inverted hierarchy case, however, $\bar{\nu}_e$ enhancement is expected to occur. The fundamental difference between ν_e and $\bar{\nu}_e$ interactions, for example, CC cross-sections and $d\sigma/dy$ distributions where y is the Feynman y, allows statistical separation of ν_e and $\bar{\nu}_e$ interactions to examine the mass hierarchy. With a full 10-year period of data taking, the significance for the mass hierarchy determination is expected to reach 3σ or greater if $\sin^2 2\theta_{13}$~0.1. Moreover, the octant of $\sin^2\theta_{23}$ can be determined to more than 90% CL if $\sin^2 2\theta_{23} < 0.99$.

The experimental search for nucleon decays by large detectors, which has been performed for more than three decades and gave stringent constraints on the grand

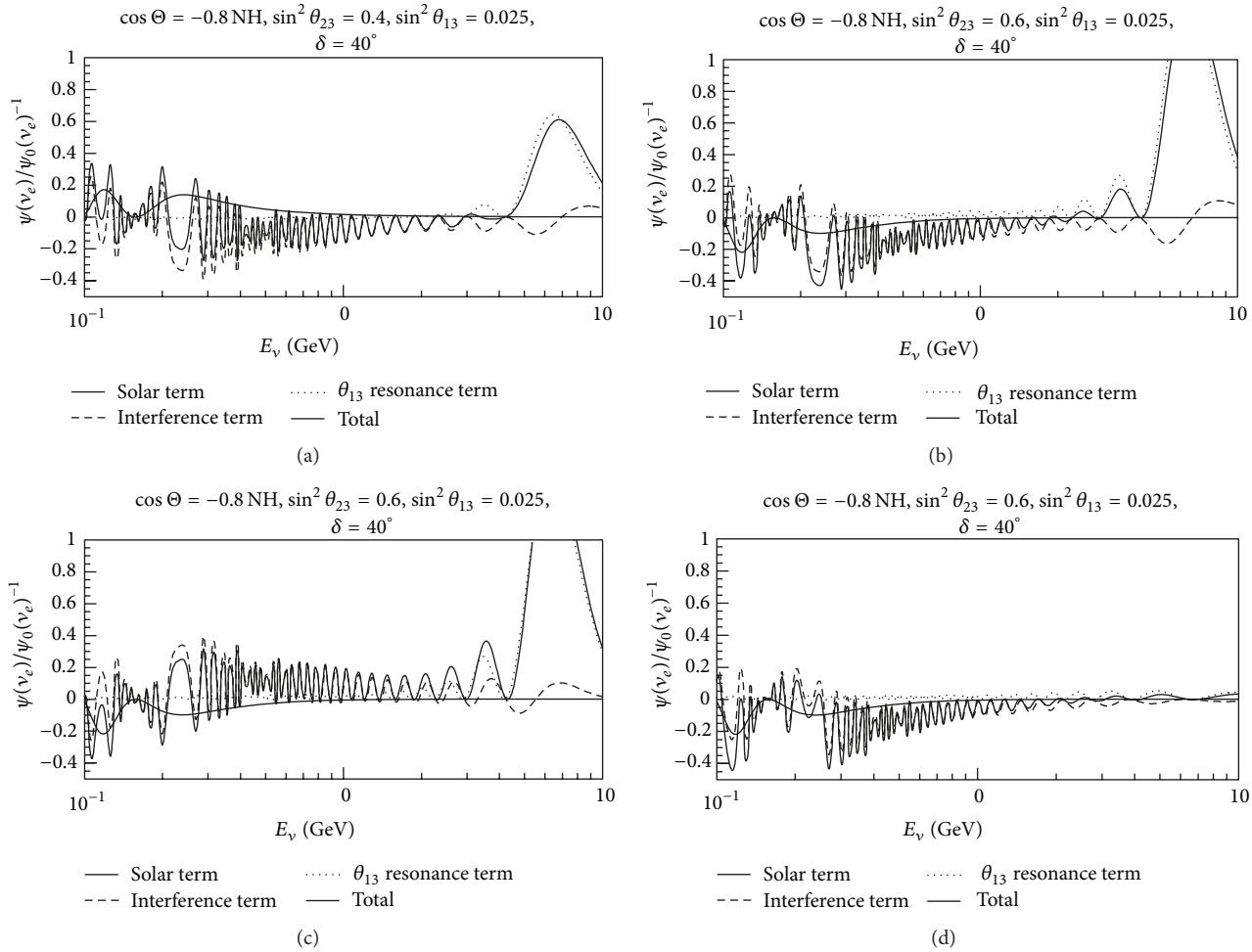

FIGURE 17: Oscillated ν_e flux relative to the nonoscillated flux as a function of neutrino energy for the upward-going neutrinos with zenith angle $\cos\Theta_\nu = -0.8$. $\overline{\nu}_e$ is not included in the plots. Thin solid lines, dashed lines, and dotted lines correspond to the solar term, the interference term, and the θ_{13} resonance term, respectively. Thick solid lines are total fluxes. Parameters are set as $(\sin^2\theta_{12}, \sin^2\theta_{13}, \sin^2\theta_{23}, \delta, \Delta m^2_{21}, \Delta m^2_{32}) = (0.31, 0.025, 0.6, 40^\circ, 7.6 \times 10^{-5}\ \text{eV}^2, +2.4 \times 10^{-3}\ \text{eV}^2)$ unless otherwise noted. The mass hierarchy is normal in (a), (b), and (c); so θ_{13} resonance (MSW) effect appears in 5–10 GeV neutrino energy region. For the inverted hierarchy case in (d), the MSW effect should appear in the $\overline{\nu}_e$ flux, which is not shown in the plot. The θ_{23} octant effect can be seen by comparing (a) ($\sin^2\theta_{23} = 0.4$) and (b) ($\sin^2\theta_{23} = 0.6$). δ value is changed to 220° in (c) to be compared with 40° in (b).

unification picture of elementary particles, is also one of major goals of the Hyper-K project. Hyper-K extends the sensitivity to nucleon decays far beyond that of Super-K. The sensitivity to the partial lifetime of protons for the decay mode $p \to e^+ + \pi^0$, the mode considered to be most model-independent, is expected to be 1.3×10^{35} years at 90% CL and 5.7×10^{34} years at 3σ CL with 10 years of Hyper-K data. This is the only realistic detector option known today able to reach this sensitivity. The 3% resolution of reconstructed proton mass by the water Cherenkov detector enhances its discovery potential for this decay mode. The sensitivity for the decay mode $p \to \overline{\nu} + K^+$, the mode favored if some supersymmetric model is correct, is also extended to 2.5×10^{34} years at 90% CL and 1.0×10^{34} years at 3σ CL.

Hyper-K also serves as an astrophysical neutrino observatory and explores the inside of stars by using neutrinos as a probe. Hyper-K will examine the possible flux variation of neutrinos from the Sun by detecting 200 solar neutrinos per day above 7 MeV total neutrino energy. If a Supernova explosion happens at the center of our galaxy, Hyper-K will accumulate 170,000–260,000 neutrinos in 10-second burst period. Even for a far Supernova at M31 (Andromeda galaxy), Hyper-K expects to collect 30–50 neutrinos. Hyper-K will provide precious data for Supernova and reveal the core collapse and explosion mechanism of massive stars. Moreover, neutrino arrival time distributions from Supernova will give constraints on the absolute neutrino mass with an expected sensitivity of 0.5–1.3 eV/c^2 that does not depend on whether the neutrino is a Dirac or Majorana particle. For Supernova relic neutrinos, in which the history of heavy element synthesis in the universe is encoded, Hyper-K expects to observe 300 neutrinos above 20 MeV in 10 years of observation. This

Table 6: Detector parameters of the baseline design.

Detector type		Ring-imaging water Cherenkov detector
Candidate site	Address	Tochibora mine
		Kamioka town, Gifu, Japan
	Lat.	$36^\circ 21' 08.928'' \mathrm{N}$
	Long.	$137^\circ 18' 49.688'' \mathrm{E}$
	Alt.	508 m
	Overburden	648 m rock (1,750 m water equivalent)
	Cosmic ray muon flux	$1.0\sim2.3 \times 10^{-6}$ sec^{-1} cm^{-2}
	Off-axis angle for the J-PARC ν	2.5° (same as Super-Kamiokande)
	Distance from the J-PARC	295 km (same as Super-Kamiokande)
Detector geometry	Total volume	0.99 megaton
	Inner volume (fiducial volume)	0.74 (0.56) megaton
	Outer volume	0.2 megaton
Photomultiplier tubes	Inner detector	99,000 20 inch ϕ PMTs
		20% photocoverage
	Outer detector	25,000 8 inch ϕ PMTs
Water quality	Light attenuation length	>100 m at 400 nm
	Rn concentration	<1 mBq/m^3

Table 7: Expected detector performance of Hyper-Kamiokande.

	Resolution or efficiency
Vertex resolution	
at 500 MeV/c	28 cm (electron)/23 cm (muon)
at 5 GeV/c	27 cm (electron)/32 cm (muon)
Particle ID	
at 500 MeV/c	$98.5 \pm 0.6\%$ (electron)/$99.0 \pm 0.2\%$ (muon)
at 5 GeV/c	$99.8 \pm 0.2\%$ (electron)/$100^{+0.0}_{-0.4}\%$ (muon)
Momentum resolution	
at 500 MeV/c	5.6% (electron)/3.6% (muon)
at 5 GeV/c	2.0% (electron)/1.6% (muon)
Electron tagging	
from 500 MeV/$c\mu^+$ decays	98%
from 5 GeV/$c\mu^+$ decays	58%
J-PARC ν_e signal efficiency	64% (nominal)/50% (tight)
J-PARC ν_μ CC background rejection	>99.9%
J-PARC $\nu\pi^0$ background rejection	95% (nominal)/97.6% (tight)
$p \to e^+ + \pi^0$ efficiency ($w/\ \pi^0$ intranuclear scattering)	45%
Atmospheric ν background	1.6 events/Mton/year
$p \to \overline{\nu} + K^+$ efficiency by prompt γ tagging method	7.1%
atmospheric ν background	1.6 events/Mton/year
$p \to \overline{\nu} + K^+, K^+ \to \pi^+ + \pi^0$ efficiency	6.7%
atmospheric ν background	6.7 events/Mton/year
Vertex resolution for 10 MeV electrons	90 cm
Angular resolution for 10 MeV electrons	30°
Energy resolution for 10 MeV electrons	20%

Table 8: Physics targets and expected sensitivities of the hyper-Kamiokande experiment updated from [2]. σ_{SD} is the WIMP-proton spin-dependent cross-section.

Physics target	Sensitivity	Conditions
Neutrino study w/J-PARC ν		
(i) CP phase precision	<20°	at $s^2 2\theta_{13} (\equiv \sin^2 2\theta_{13}) > 0.03$ and mass hierarchy (MH) is known
(ii) CPV 3σ discovery coverage	74%	at $s^2 2\theta_{13} = 0.1$, 7.5 MW·yrs MH known
	54%	at $s^2 2\theta_{13} = 0.1$, 7.5 MW·yrs MH unknown
	69%	at $s^2 2\theta_{13} = 0.1$, 3.75 MW·yrs MH known
	42%	at $s^2 2\theta_{13} = 0.1$, 3.75 MW·yrs MH unknown
Atmospheric neutrino study		10-year observation
(i) MH determination	$>3\sigma$ CL	at $0.4 < s^2\theta_{23}$ and $0.04 < s^2 2\theta_{13}$
(ii) θ_{23} octant determination	>90% CL	at $s^2 2\theta_{23} < 0.99$ and $0.04 < s^2 2\theta_{13}$
Nucleon decay searches		10 years data
(i) $p \rightarrow e^+ + \pi^0$	1.3×10^{35} yrs (90% CL) 5.7×10^{34} yrs (3σ CL)	
(ii) $p \rightarrow \overline{\nu} + K^+$	2.5×10^{34} yrs (90% CL) 1.0×10^{34} yrs (3σ CL)	
Solar neutrinos		
(i) ^{8}B ν from Sun	200 ν's/day	7.0 MeV threshold (total energy)
(ii) ^{8}B ν day/night accuracy	<1%	5 years, only stat. error
Astrophysical objects		
(i) Supernova burst ν	170,000–260,000 ν's	at Galactic center (10 kpc)
	30–50 ν's	at M31 (Andromeda galaxy)
(ii) Supernova relic ν	300 ν's/10 years	>20 MeV
(iii) WIMP annihilation at Sun		5-year observation
	$\sigma_{SD} = 10^{-39}$ cm^2	at $M_{WIMP} = 10$ GeV $\chi\chi \rightarrow b\bar{b}$ dominant
	$\sigma_{SD} = 10^{-40}$ cm^2	at $M_{WIMP} = 100$ GeV $\chi\chi \rightarrow W^+W^-$ dominant

large sample will enable us to explore the evolution of the universe. By doping Gadolinium salt in the detector water, the delayed gamma signal for the inverse beta decay of relic neutrinos—$\overline{\nu}_e + p \rightarrow e^+ + n$ and the reaction Gd$(n, \gamma s)$ Gd—enable us to much reduce the backgrounds and open up the signal energy window below 20 MeV. The expected signal in the 10–30 MeV energy region is 830 neutrinos in 10 years of Hyper-K. Another astrophysical target in Hyper-K is possible neutrinos emitted by weakly interacting massive particles (WIMPs) annihilating or decaying in the Sun, Earth, and galactic halo. Sensitivity to the WIMP-proton spin-dependent cross-section would reach $10^{39}(10^{40})$ cm^2 for a WIMP mass of 10 (100) GeV. Other astronomical neutrino searches such as solar flare neutrinos, GRB neutrinos, and galactic diffuse neutrinos can be also performed in Hyper-K.

4. The European Approach

4.1. EUROnu. EUROnu is a design study within the European Commission Seventh Framework Program, Research Infrastructures. It is investigating the three possible options for a future, high-intensity neutrino oscillation facility in Europe. The aim is to undertake conceptual designs for the facilities, determine the performance of the corresponding baseline detectors, and compare the physics reach and cost of the facilities. The work is being undertaken by the EUROnu

consortium, consisting of 15 partners and a further 15 associate partners [34].

The three facilities being studied are as follows.

(i) The CERN to Fréjus Super Beam, using the 4 MW version of the Superconducting Proton Linac (SPL) at CERN [35]. The baseline far detector is a 500 kT fiducial mass water Cherenkov detector, MEMPHYS [36].

(ii) The Neutrino Factory, in which the neutrino beams are produced from the decay of muons in a storage ring. This work is being done in close collaboration with the International Design Study for a Neutrino Factory (IDS-NF) [37].

(iii) The Beta Beam, in which the neutrino beams are produced from the decay of beta emitting ions, again stored in a storage ring.

The project started on September 1, 2008 and will finish on August 30, 2012, and thus, is very advanced at the time of writing. The work done on the accelerator facilities, the detectors, and in determining the physics performance will be described in the following subsections.

4.1.1. The Super Beam. A Super Beam creates neutrinos by impinging a high-power proton beam onto a target and focussing the pions produced towards a far detector using a magnetic horn. The neutrino beam comes from the pion decay (Figure 18). EUROnu is studying the CERN to Fréjus Super Beam, using the high-power superconducting proton Linac (HP-SPL) [35] as the proton driver, producing a 4 MW beam. The baseline is 130 km and the planned far detector is the 500 kT fiducial mass MEMPHYS water Cherenkov detector [36] in the Fréjus tunnel. The main activities consisted in designing and testing candidate targets and magnetic horns, integrating the targets and horns together, studying the required target station, designing the proton beam handling system beyond the SPL, and determining the characteristics of the resulting neutrino beam for physics simulations.

Given the difficulty in producing a single target and horn able to work in a 4 MW beam, the option taken in EUROnu is to use four of each instead. The beam will then be steered on to each target in turn, so that they all run at 12.5 rather than 50 Hz and receive 1 MW. For the targets and the horns, this results in a smaller extrapolation from technology already in use. An outline design for the 4 target and horn system is shown in Figure 18. The baseline design for the target is a pebble bed, consisting of 3 mm diameter spheres of titanium in a canister. These are cooled by flowing helium gas through vents in the canister. Modeling suggests that a sufficient flow rate can be achieved to cool the targets, even with a higher-power beam. Nevertheless, offline tests of the cooling system, using an inductive heating coil, are planned. A test target will also be subjected to a beam of the correct energy density using the HiRadMat [38] facility at CERN. The horn design is based on that of the MiniBooNE experiment [39] and will not have a reflector. The design has been modified to optimize the pion production. The horns will need to be pulsed at least 300 kA, resulting in significant heating

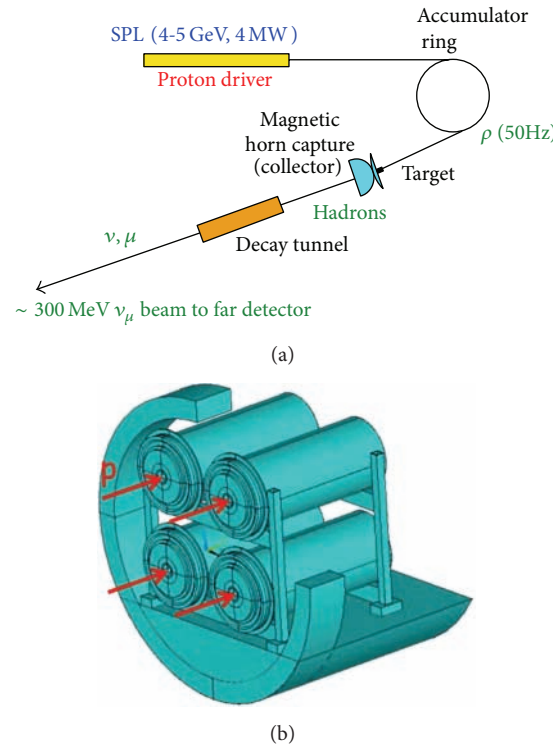

Figure 18: (a) Layout of the CERN to Fréjus Super Beam. (b) Conceptual engineering design of the 4 target and horn system for the Super Beam.

from both the current and beam loss, corresponding to a maximum of 12 kW on the surface closest to the target. Modeling suggests that this can be removed with sufficient water cooling. The thermal stresses in the target material are a maximum of 18 MPa and prototype tests will be required to determine the lifetime due to fatigue and radiation damage. A support system for the 4 horn system under this load has, however, been designed. Finally, a prototype pulsing circuit has been designed and will be built and tested. An initial design of the target station has also been made, based on radiation and activation studies. This incorporates the necessary shielding and remote handling for 4 MW and also has storage for the old targets and horns.

The final area studied is the beam delivery from the SPL to the target. As shown in Figure 18, this requires an accumulator ring to reduce the large number of bunches from the linac to a small number for delivery to the target. An initial design of this ring has been made. In addition, a design for the system to split the beam on to the 4 targets has been made and the engineering aspects of this are under study.

4.1.2. The Neutrino Factory. In a Neutrino Factory, the neutrinos are produced from the decay of muons in a storage ring. The muons are produced by impinging a 4 MW proton beam onto a heavy metal target and focussing the pions produced into a decay channel using a 20 T superconducting solenoid. In the original baseline, the muons from the pion decay are captured, bunched, phase rotated, and finally cooled in the muon front-end, before being accelerated using a

linac, two recirculating linear accelerators (RLAs) and a nonscaling fixed-field alternating gradient accelerator (ns-FFAG) to 0.9 GeV, 3.6 GeV, 12.6 GeV, and 25 GeV, respectively (see Figure 19). The muons are then injected into two storage rings, to produce beams of neutrinos and antineutrinos to two far detectors.

However, following the measurement of θ_{13}, the required muon energy has been reduced to 10 GeV and only one decay ring will be used. The envisaged neutrino baseline is now around 2000 km.

The work in this project is being done in close collaboration with the International Design Study for a Neutrino Factory (IDS-NF) [37]. However, EUROnu is focussing on the section from the pion production target to the muon acceleration system. The baseline target is a liquid mercury jet. However, modeling done in EUROnu has shown that the heat load from the secondaries produced in the superconducting solenoids used to focus the pions is much too big, around 50 kW. The main problem is secondary neutrons. Although this can be fixed by adding more shielding, this would double the radius of the super-conducting coils, making these significantly more difficult. A study of pion production has shown that similar production rates can be achieved with lower atomic number elements (see Figure 19), but these produce significantly fewer neutrons. As a result, targets with lower atomic number are under study. An interesting candidate is gallium, which has a low enough melting point that it could be used as a liquid.

A related issue is the transmission of secondaries into the muon front-end. As well as the required large flux of muons, there are also still many protons, pions, and electrons. If nothing is done about these, they will be lost throughout the front-end, resulting in levels of activation about 100 times above the canonical level for hands-on maintenance. The front-end is being redesigned in EUROnu to include a chicane, to remove the higher momentum unwanted particles, and an absorber, to remove those at lower momentum. The efficiency for transmission of useful muons is about 90%, while the unwanted particles are reduced to a manageable level. This scheme has recently been incorporated in the neutrino factory baseline.

For the cooling channel, an engineering demonstration of the cooling technique, ionization cooling, is being constructed at the STFC Rutherford Appleton Laboratory. This project, called MICE [40], is due to give a first demonstration of ionisation cooling during 2013. In addition, the RF cavities of the baseline cooling cell will be in a large magnetic field, resulting from the coils used to focus the beam to increase the cooling efficiency. Measurements done in the MuCool project [41] suggest this could limit the accelerating gradient before the cavities breakdown. Alternative cooling lattices have been studied in EUROnu that reduce the magnetic field at the cavities, while maintaining the same performance. One of these is under consideration to become the new baseline for the cooling channel.

The design of the acceleration system is well advanced, though full 6D tracking still needs to be done. Following the reduction to 10 GeV, two options now exist for this system. The first uses a linac and two RLAs, while the second replaces the higher-energy RLA with a ns-FFAG. Both options are under study to determine which would be best based on performance and cost. As ns-FFAGs are an entirely novel type of accelerator, a proof-of-principle machine called EMMA [42] has been constructed at the STFC Daresbury Laboratory (see Figure 20). This has recently demonstrated that many of the novel features of the muon accelerator, in particular serpentine acceleration and multiple resonance crossings, work. The full EMMA experimental program has recently started and will study the remaining issues.

4.1.3. The Beta Beam. Production of (anti)neutrinos from beta decay of radioactive isotopes circulating in a race-track-shaped storage ring was proposed in 2002 [43]. Beta Beams produce pure ν_e or $\overline{\nu}_e$ beams, depending on whether the accelerated isotope is a β^+ or a β^- emitter. The "Beta Beam facility" is based on CERN's infrastructure and the fact that some existing accelerators can be reused will reduce the cost, though it will constrain the performance (see Figure 21).

One of the main issues studied by EUROnu is the production, acceleration, and storage of a sufficient flux of ions to meet the physics goals. The isotope pair that was first studied for neutrino production, in the EURISOL FP6 Design Study [44], is ^{6}He and ^{18}Ne, accelerated to $\gamma = 100$ in the SPS and stored in the decay ring [44]. At the end of EURISOL, the flux of ^{18}Ne that looked possible was a factor of 20 too small. This has been addressed in two ways in EUROnu. The first was to consider a production ring (12 m circumference) with an internal gas jet target [45] to make an alternative ion pair, ^{8}Li and ^{8}B. In this, a 25 MeV beam of ^{7}Li and ^{6}B is injected over a gas jet target of d and ^{3}He, respectively. Significant studies of this have been undertaken, including the measurement of the double differential cross-sections for the reactions, studies of achievable gas flow rates in the ring and the construction of a prototype device for collection of the produced isotopes (see Figure 21). These have shown that the required target gas flow would be very challenging and that it would be very difficult to achieve the required rates.

As a result, research on a novel ^{18}Ne-production method, using a molten salt loop (NaF) by the reaction ^{19}F(p,2n) ^{18}Ne, is currently being undertaken. Modeling suggests that this could achieve the required production rate with an upgrade of Linac 4 [46] at CERN from 4 to 6 mA. An experiment to demonstrate the method will take place at ISOLDE at CERN in June 2012. As a result of the work done so far, the ^{6}He and ^{18}Ne ion pair are currently the baseline for the Beta Beam.

Research and development of a 60 GHz pulsed ECR source to bunch the ions produced are continuing within EUROnu. A prototype device has been constructed and successful magnetic tests have been done. These will be followed by tests with the gyrotron and with beam. Compatibility and possible integration of Beta Beams in the upgrade program for the LHC is essential and is being actively studied. Requirements to have very short and intense bunches in the decay ring (due to signal/noise in the detector) favors beam instabilities for which solutions will be found by reoptimizing the bunch structure over the accelerator cycle.

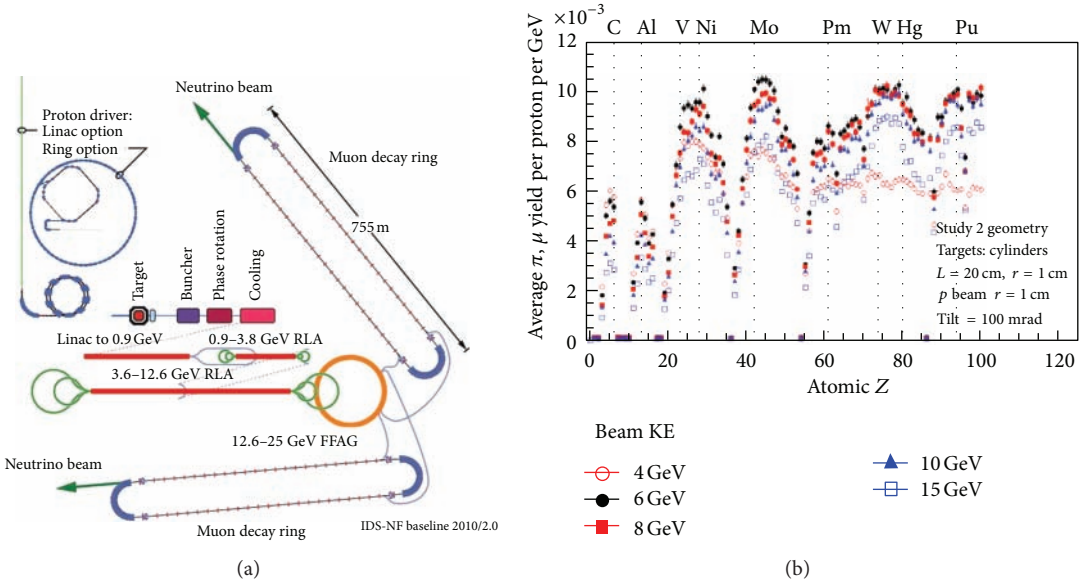

FIGURE 19: (a) Original baseline layout of the neutrino factory. (b) Pion production as a function of atomic number, assuming a cylindrical target 20 cm long and 2 cm in diameter.

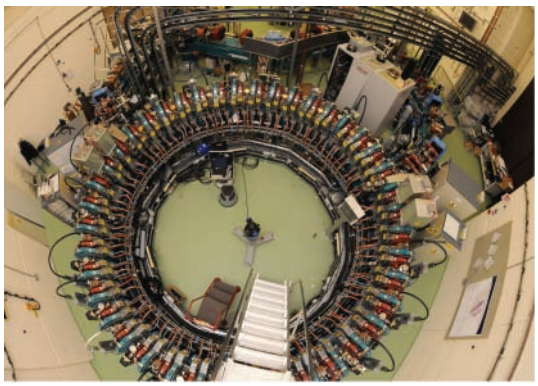

FIGURE 20: The EMMA proof-of-principle accelerator at the Daresbury Laboratory.

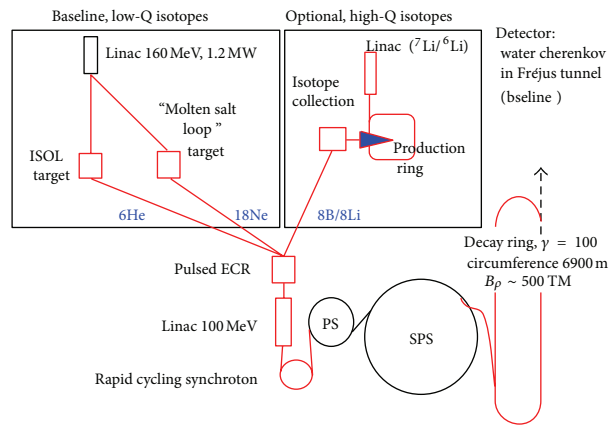

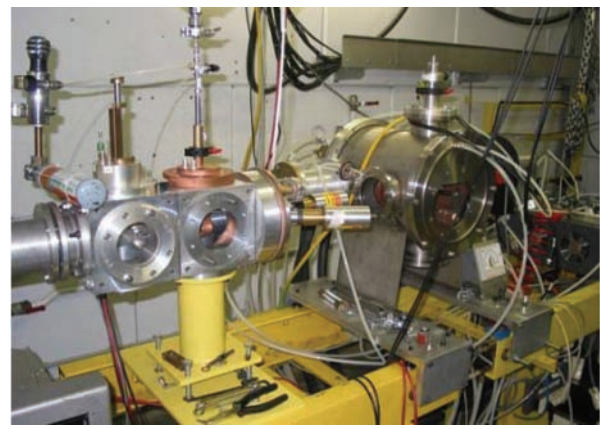

(b)

FIGURE 21: (a) Layout of the CERN Beta Beam. (b) The prototype ion collection device constructed for Beta Beam studies.

The baseline isotopes could use the MEMPHYS detector [36]. For the ^{8}Li and ^{8}B option, a detector some 700 km away would be needed.

4.1.4. Detectors. The focus of EUROnu is on the accelerator facilities. Nevertheless, to make a genuine comparison between physics performance and cost, it is also important to include the neutrino detectors in the study. Thus, the project includes the baseline detectors for each facility, with the aim of determining their performance in detecting neutrinos and the cost of construction.

The baseline for the Neutrino Factory is a magnetized iron neutrino detector (MIND). This is an iron-scintillator calorimeter, with alternating planes of 3 cm thick iron and 2 cm thick solid scintillator. One detector is now planned, of 100 kT mass at around 2000 km. This is based on the MINOS detector [47] and will have a transverse size of around 15 by

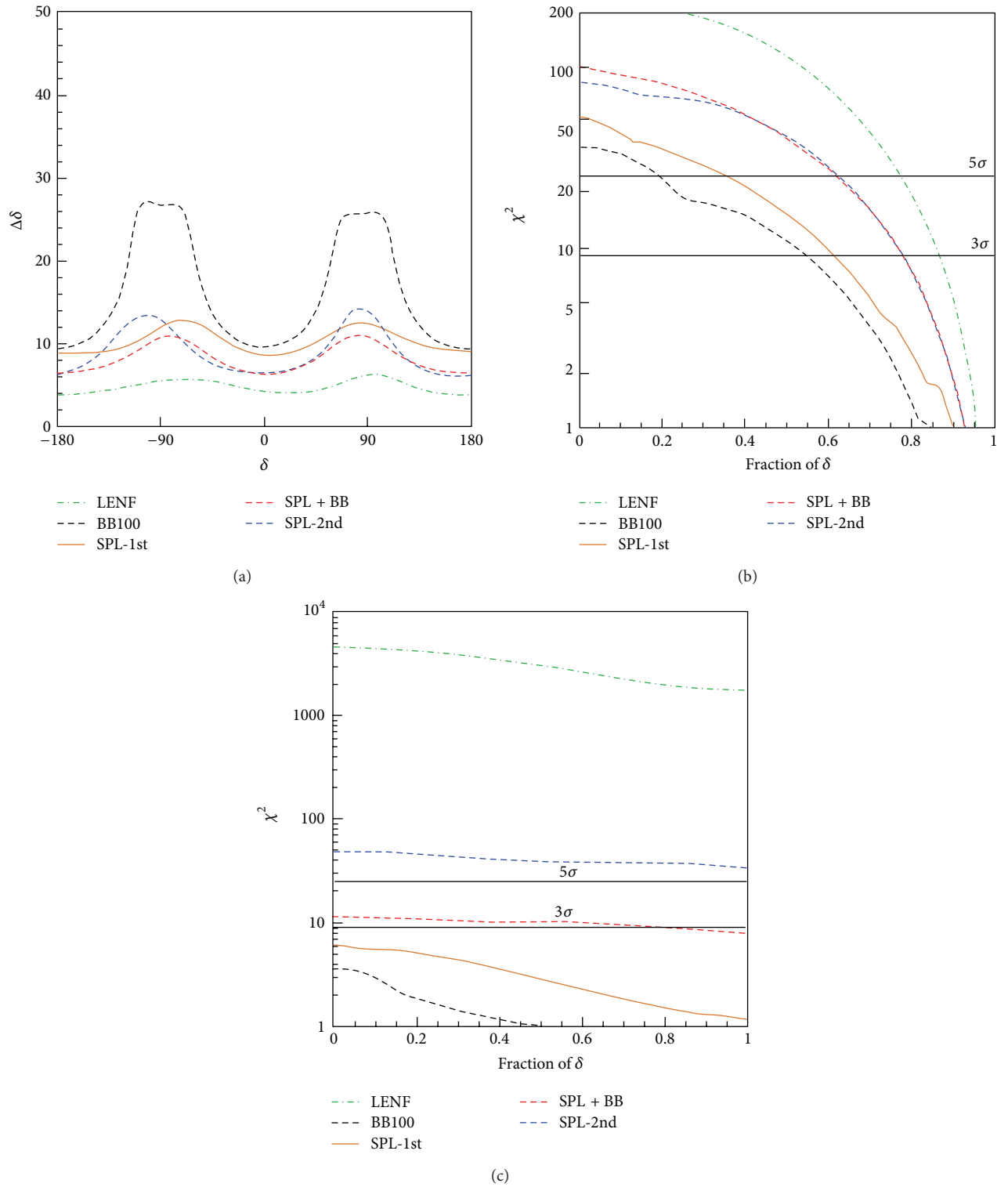

FIGURE 22: Summary of the physics performance of the facilities described in the text. (a) The 1σ measurement errors for the CP angle δ as a function of δ. (b) The range of δ for which a 3 and 5σ measurements of δ can be made. (c) The range of δ for which 3 and 5σ measurements of the neutrino mass hierarchy can be made.

15 m. The baseline for both the Super Beam and Beta Beam facilities is the MEMPHYS detector [36] in the Fréjus tunnel. This will be a 500 kT fiducial mass water Cherenkov detector. Note that using the same detector would make it possible to run the Super Beam and Beta Beam at the same time. Near detectors have also been designed for all three facilities.

4.1.5. EUROnu Physics. The physics group in EUROnu is determining the physics reach of each facility and combination of facilities using the parameters provided for the accelerators and detectors. They also assess and include the corresponding systematic errors in a uniform way and optimize performance based on information from other experiments. Following the recent indications of large θ_{13}, they have now started a physics reach comparison between the EUROnu facilities and a number of others. Preliminary examples of this work are shown in Figure 22 [48]. The facilities being considered are the following.

(i) LENF: the low-energy neutrino Factory, with a 10 GeV muon energy, 1.4×10^{21} decays per year and a single 100 kt mass MIND detector at a baseline of 2000 km.

(ii) BB100: a $\gamma = 100$ Beta Beam, with $1.3/3.5 \times 10^{18}$ decays per year of Ne/He, a 10^{-2} atmospheric background suppression, and a 500 kt water Cherenkov detector at Fréjus.

(iii) SPL-1st: a 4 MW SPL Super Beam with 500 kt water Cherenkov detector at Fréjus, corresponding approximately to the first oscillation maximum.

(iv) SPL-2nd: as above, but with the detector at Canfranc, corresponding to approximately the second oscillation maximum.

(v) SPL+BB: the combination of BB100 and SPL-1st.

For the low-energy Neutrino Factory, the signal systematic error used is 2.4%, while it is 5% for the other facilities. The systematic error used for the background in all cases is 10% and 10-year running time is assumed.

4.1.6. Costing and Safety. The EUROnu comparative costing is based on the three facilities being located at CERN, to put the costing on the same basis. Similar assumptions are being made and common costs are being used wherever possible. It is being overseen by a costing panel. To complement this, the major safety aspects and technical risks of the facilities are being assessed. As only limited resources are available, the emphasis in costing is to achieve the best relative precision between the facilities. The same principle is being applied for the safety assessment. It will use existing experience, where that exists. The technical risks will be assessed by the facilities at the end of the design study.

4.2. LAGUNA and LAGUNA-LBNO. Neutrinos are messengers from astrophysical objects as well as from the early universe and can give us information on processes, which cannot be studied otherwise. Underground experiments, like Super-Kamiokande (SK) [49], have made important discoveries. Next-generation very-large-volume underground experiments will answer fundamental questions on particle and astroparticle physics. The construction of a large-scale detector devoted to particle and astroparticle physics in Europe is one of the priorities of the ASPERA [50] roadmap (2008). These detectors will search for a possible finite lifetime for the proton with a sensitivity one order of magnitude better than the current limit. With a neutrino beam they will measure in a complementary way the mixing angle (θ_{13}) of neutrinos, the hierarchy of the mass eigenstates and unveil through neutrino oscillations the existence of CP violation in the leptonic sector, which in turn could provide an explanation of the matter-antimatter asymmetry in the Universe. Moreover, they will study astrophysical objects, in particular the Sun and Supernovae [51, 52]. The FP7 Design Studies LAGUNA (2008–2011) [53–55] and LAGUNA-LBNO (2011–2014) [56] support studies of European research infrastructures in deep underground cavities able to host a very large multipurpose next-generation neutrino observatory—GLACIER (liquid argon) [57], lENA (liquid scintillator) [58], and MEMPHYS (water Cherenkov) [36, 59].

The FP7 Design Study LAGUNA (2008–2011) was a Pan-European effort of 21 beneficiaries, composed of academic institutions from Denmark, Finland, France, Germany, Poland, Spain, Switzerland, and UK, as well as industrial partners specialized in civil and mechanical engineering and rock mechanics. The goal of the study was to assess the feasibility of this research infrastructure in Europe and the related costs.

The LAGUNA consortium has evaluated possible extensions of the existing deep underground laboratories in Europe: Boulby (UK), Canfranc (Spain), and Modane (France) and considered the creation of new laboratories in the following sites: *Caso* Umbria Region (Italy), *Pyhäsalmi* (Finland), *Sieroszowice* (Poland), and *Slanic* (Romania). In Europe there are three different proposed detectors: GLACIER, LENA, and MEMPHYS. For all three detectors there are, in the LAGUNA context, specific studies concerning the construction feasibility, the required depth, the muon and reactor neutrino flux, and so forth. In Figure 23, the seven sites are shown, as well as an example of the construction studies developed by the different beneficiaries. The main conclusion of the LAGUNA study is that from a rock mechanical point of view all the proposed excavations are possible. Detailed cost estimations for the site construction and estimations for the detector constructions have been delivered. It turned out that the cavern construction itself is not the most important cost driver in such future project. In order to make a realistic overall cost estimation, the detector construction costs and the costs related to the operation of the infrastructure for at least 30 years or more have to be studied in more detail. Furthermore, the physics potential of each combination of site and detector has to be investigated in detail and in a common way. This led the collaboration to propose the second phase study: LAGUNA-LBNO, which was accepted within the European FP7 framework.

The LAGUNA collaboration decided to go ahead with a new study, LAGUNA-LBNO (2011–2014) to investigate two

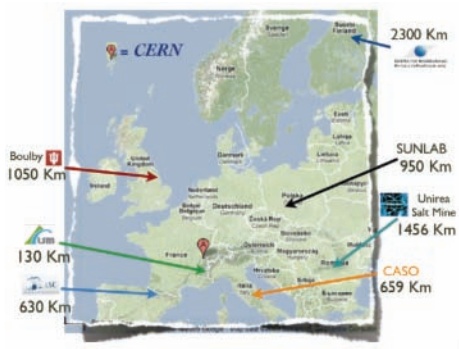

(a)

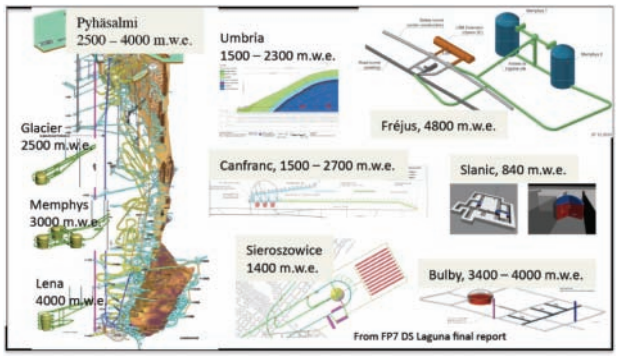

(b)

FIGURE 23: (a) Map of the seven possible underground sites in Europe. (b) Exemplary layouts studied in LAGUNA DS for each site.

sites in detail: the shortest baseline from CERN, Fréjus at 130 km with no matter effect and therefore providing a clean measurement of CP violation and the longest baseline at Pyhäsalmi (2300 km) with matter effects and therefore able to determine the mass hierarchy. A third site, Umbria in Italy at 730 km from CERN, is investigated with lower priority. Umbria is a green field location in the existing CERN-CNGS beam.

LAGUNA-LBNO is a collaboration of about 300 physicists and engineers from 13 countries including 39 research institutions and industrial partners. Two non-European countries, Japan and Russia, are partners of the project. LAGUNA-LBNO will provide a realistic scheme for the tank construction and the costing of the detector itself. The costs involved with liquid procurement and long-term running of the new underground laboratory will be evaluated. New beam options based on the existing CERN accelerator complex are investigated and the physics potential of each detector option at the two locations will be studied.

At the Pyhäsalmi site, two options are studied: a 50 kt liquid scintillator detector (LENA) and the GLACIER detector with 20 kt and 50 kt liquid argon for a staged instrumentation. Both detectors are located at a depth of roughly 4000 m.w.e. For the Fréjus site, the MEMPHYS project in combination with a β-Beam (βB) or a Superbeam (SB) from CERN is under investigation. In parallel, a hybrid option of one or two MEMPHYS tanks together with the LENA experiment will be investigated [60].

4.3. The Three Detectors: GLACIER, LENA, and MEMPHYS. The *GLACIER* (Giant Liquid Argon Charge Imaging Experiment) detector is based on a new liquid argon detector concept, scalable to a single unit of mass 100 kt: it relies on a cryogenic storage tank developed by the petrochemical industry (LNG technology) and on a novel method of operation called the LAr LEM-TPC. LAr LEM-TPCs operate in double phase with charge extraction and amplification in the vapor phase. The concept has been very successfully demonstrated on small prototypes: ionization electrons, after drifting in the LAr volume, are extracted by a set of grids into the gas phase and driven into the holes of a double-stage Large Electron Multiplier (LEM), where charge amplification occurs.

Effective extrapolation to the required scale needs concrete R&D. A ton-scale LAr LEM-TPC detector has been successfully operated at CERN in Blg 182 within the CERN RE18 experiment (ArDM). The detector has been moved to the Canfranc underground laboratory in Spain to search for direct WIMP signals. In order to prove the performance for neutrino physics, additional dedicated test beam campaigns are being considered, to test and optimize the readout methods and to assess the calorimetric performance of such detectors. A 1 kt detector can be built assuming the GLACIER design with a 12 m diameter and 10 m vertical drift. The layout of the GLACIER tank and its implementation in the Pyhäsalmi mine is shown in Figure 24.

Thanks to the very good imaging capabilities of the GLACIER detector in combination with a neutrino beam from CERN the experiment has outstanding physics potential. The high resolution of the detector allows the precise measurement of the first and second oscillation maximum and therefore the precise determination of θ_{13}, the CP violating phase δ, and the mass hierarchy.

As stated above, the GLACIER experiment is scalable and therefore a staged approach is actively developed. The first phase is a 20 kt double phase LAr LEM-TPC (GLACIER) combined with a magnetized muon detector (MIND). The beam is based on a conventional neutrino beam line with a baseline of 2300 km towards Pyähsalmi, Finland (CN2PY) with protons from an upgraded CERN SPS (700 kW). An Expression of Interest has been submitted to the CERN SPSC for this project [62].

The experiment allows the precise determination of oscillation parameters by measuring all transition probabilities ($\nu_\mu \to \nu_\mu, \nu_\mu \to \nu_\tau, \nu_\mu \to \nu_e$) with neutrinos and antineutrinos. It can achieve a precise determination of the neutrino mass hierarchy (5σ CL) within a few years. In about 10 years, 60% of the CP violation parameter space will be covered at 90% CL In Figure 25, we show in the left panel the 68% and 90% CL contours for δ_{CP} and in the right panel the potential to determine the mass hierarchy.

Thanks to the deep underground location, this initial phase can reach a number of outstanding physics goals.

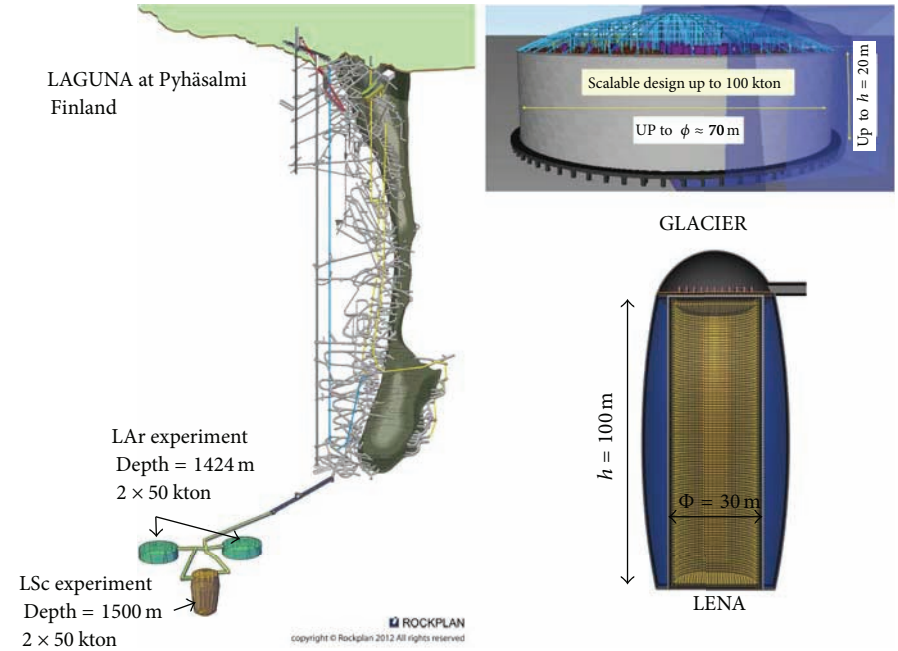

Figure 24: Schematic view of the Pyhäsalmi mine and the GLACIER and LENA detector with their access shafts.

The new underground neutrino observatory addresses the unification of elementary forces by searching for nucleon decay. The limit on the proton lifetime will be improved to $\tau_p \geq 2 \times 10^{34}$ years in the channel $p \to K\overline{\nu}$ at 90% CL. The first stage of GLACIER will contribute with major advances in the multimessenger neutrino astronomy with the detection of astrophysical and terrestrial neutrinos (solar, atmospheric neutrinos) and dark matter annihilation. GLACIER can detect neutrino bursts from galactic and extragalactic supernova which can unveil the mechanisms of the stellar collapse. For a supernova explosion at 10 kpc, 10,000 neutrino interactions will be recorded. Furthermore, 5600 atmospheric neutrino events per year will be measured.

In a second phase (≥2025), the detector can be upgraded to reach the full seize of 100 kt and the beam power will be increased with a HP-PS (2 MW) or a neutrino factory, for example, which allows 75% coverage of the CP violation parameter space at 3σ CL [63].

The *LENA* (Low-Energy Neutrino Astronomy) detector design foresees the use of 50 kt of liquid scintillator (LSc) for neutrino detection. The LSc will be contained in a cylindrical concrete tank of 32 m diameter and 100 m height. Inside the detector tank, a scaffolding, optically separated from the tank walls will be installed as a framework for optical modules (OMs) facing the interior of the detector at a radius of 14 m. The PMT support structure is depicted in Figure 26(a).

The optical modules will contain $12''$ PMTs equipped with Winston cones for light collection. They will be fully encapsulated for pressure resistance with an enclosed buffer of non-scintillating oil to impede γ-radiation from the PMT glass from reaching the scintillator. The setup of an OM is shown in Figure 26(b). The design foresees the installation of 29600 OMs leading to an optical coverage of 30%.

The detector tank has to be placed in an underground cavern to provide shielding from cosmic radiation. The design foresees a volume around the detector tank to be filled with pure water acting as a Cherenkov veto for cosmic muons as well as a shielding for fast neutrons. The preferred locations are either in the Pyhäsalmi mine in central Finland, at a depth of 1400 m (4000 m.w.e.), or in the Laboratoire Souterrain de Modane adjacent to the Fréjus tunnel in the French-Italian Alps with a rock overburden corresponding to 4800 m.w.e. A detailed description of the LENA project can be found in [64].

The concept of neutrino spectroscopy has been successfully demonstrated by both KamLAND and Borexino. The low-energy threshold of LSc offers a wide range of physics based on neutrinos from terrestrial and astrophysical sources. The core research program will be the detection of neutrinos with energies reaching from sub-MeV to tens of MeV, but LENA can also contribute to several aspects of neutrino and particle physics associated to GeV energies.

The huge target mass of LENA gives the opportunity of a high statistics spectral measurement of the solar neutrino flux. Approx. 10^4 solar neutrino interactions per day allow for a measurement of the ^{7}Be neutrino flux with an unprecedented accuracy. This offers the opportunity to search for temporal variations in the flux and thus to probe the effects of possible helioseismic g-modes [65]. A measurement of the up to now undetermined CNO neutrino flux would provide valuable information on the solar metallicity and fusion processes in the solar center. The high statistics spectral measurement of solar neutrinos will allow for a precise

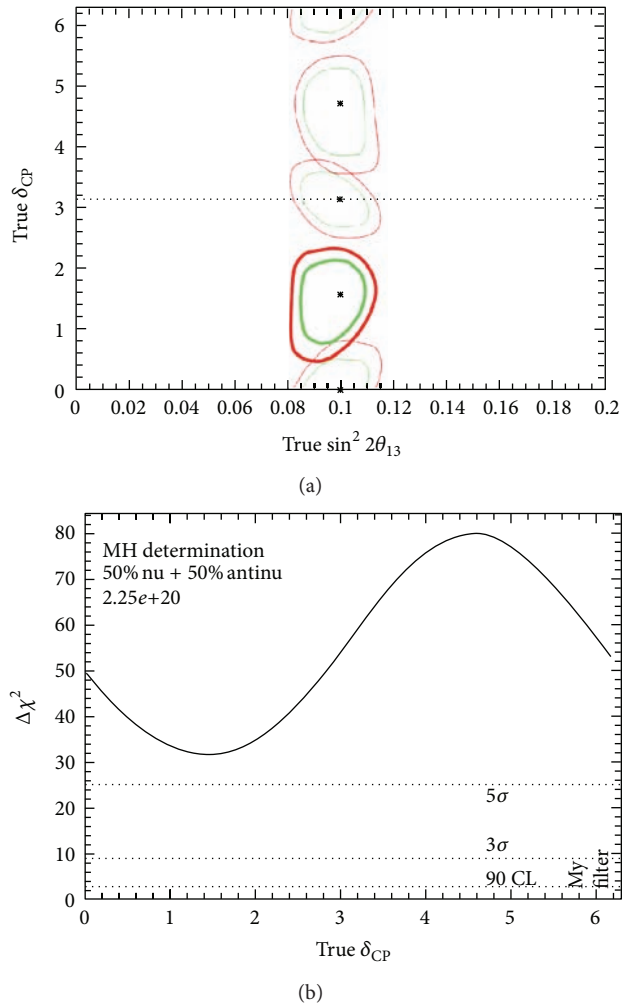

FIGURE 25: (a) The 68% and 90% CL contours in the δ_{CP}-$\sin^2 2\theta_{13}$ plane. (b) Mass hierarchy determination at 5σ [61].

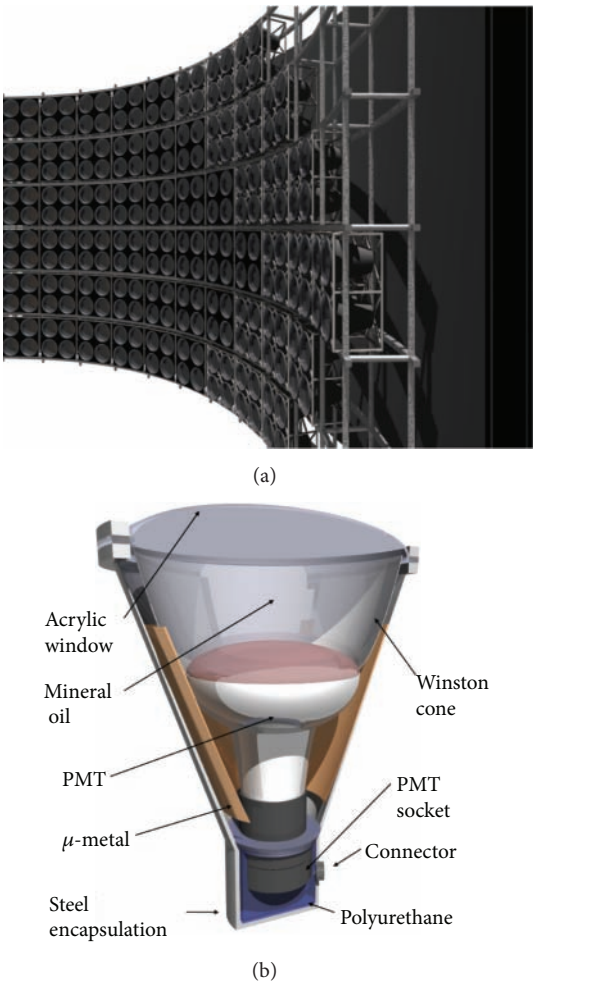

FIGURE 26: (a) The PMT support structure is optically shielded from the tank walls; (b) each optical module contains a fully enclosed PMT equipped with a Winston cone. Nonscintillating mineral oil is added to prevent gammas emerging from the PMTs from reaching the scintillator [64].

determination of the ν_e survival probability in the transition region between vacuum and matter dominated oscillations.

LENA offers excellent capabilities for the observation of a galactic core-collapse Supernova [64]. Different neutrino detection channels offer the opportunity to determine individual, time-dependent spectra for different neutrino types and thus allow for an energy and flavor resolved real-time analysis. For a standard Supernova in the center of our galaxy approx. 10^4 events are expected within a few seconds. These are predominately $\overline{\nu}_e$ interactions; however, there will also be a large signal from ν_μ and ν_τ scattering on protons.

While the predicted rate of galactic Supernovae is about one to three per century, the isotropic neutrino background from Supernovae on cosmic scales is expected to provide a flux of approx. 100 $\nu/\text{cm}^2\text{s}$. This so-called diffuse Supernova neutrino background (DSNB) has not yet been observed. Based on current models, LENA is almost certain to detect the $\overline{\nu}_e$ component of the DSNB by looking in the energy window between 10 and 30 MeV formed by the reactor neutrino and atmospheric neutrino background. The expected event rate is of the order of 2 to 20 events per year, depending on the underlying Supernova model and Supernova rate [67].

The inverse beta decay offers an excellent detection channel for $\overline{\nu}_e$ in LENA not only for Supernova physics. Because of the coincidence signal of the positron and the delayed neutron capture, this channel is virtually background-free. Due to the low detection threshold of 1.8 MeV, LENA will also be sensitive to geoneutrinos, expecting roughly 1000 events per year [68]. Geoneutrinos are produced in the decay of radioactive isotopes in the Earth's core, mantle, and crust. Measuring their spectra allows to determine the abundances of ^{238}U and ^{232}Th and their natural decay chains. The measurement of reactor $\overline{\nu}_e$ offers the opportunity for precision measurement of Δm^2_{12} [69].

Furthermore, LENA allows for an indirect search for dark matter (DM) by observing neutrinos produced in the annihilation or decay of DM particles. LENA is especially sensitive in the region of 10 to 100 MeV which is not easily accessed by other experiments.

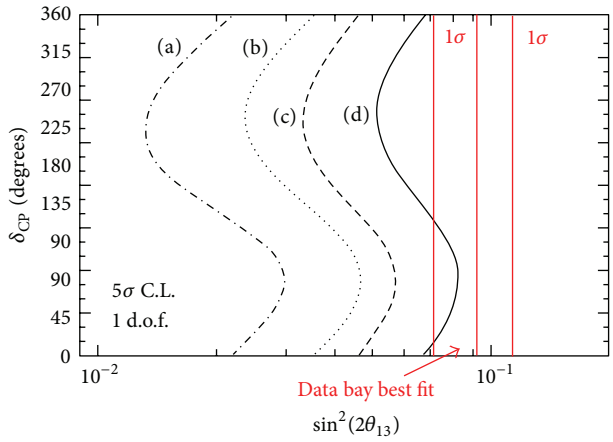

(a) 3×10^{21} pot/yr; 50% CC-10% NC
(b) 1×10^{21} pot/yr; 50% CC-10% NC
(c) 3×10^{21} pot/yr; 27% CC-11% NC
(d) 1×10^{21} pot/yr; 27% CC-11% NC

FIGURE 27: Sensitivity of LENA to the neutrino mass hierarchy for the 2288 km long-baseline CERN to Pyhäsalmi and for different detector and beam performances at 5σ CL Detector performance parameters like the NC rejection efficiency are still under investigation [66].

Within LAGUNA-LBNO, the use of LENA as a target for a possible future neutrino beam is currently under investigation [71]. A realistic scenario is the use of a conventional $\nu_\mu/\overline{\nu}_\mu$-beam from CERN. Located in the Pyhäsalmi mine in central Finland, the LENA detector will be at a baseline distance to CERN of 2288 km. This corresponds to the first oscillation maximum of a ν_μ beam with an energy of 4.2 GeV. By searching for the appearance of ν_e in the ν_μ beam, LENA can shed new light on the neutrino mass hierarchy and the neutrino mixing parameter δ_{CP}. Figure 27 shows the sensitivity to the mass hierarchy. For the recently determined central value of θ_{13}, LENA could determine the mass hierarchy at the 5σ CL level.

To reconstruct the complex vertices created by the interactions of GeV neutrinos, a reliable tracking and identification of all final state particles is needed. The possibility of particle tracking in unsegmented LSc detectors is currently investigated in a great effort, returning promising results on the neutrino energy reconstruction and NC background identification.

The NC/CC discrimination applied in this analysis relies on pulse shape analysis/tagging of muon decay electrons to suppress NC background events featuring charged pions and on a multivariate analysis (again relying mostly on pulse shape parameters) to distinguish π^0 NC form ν_e CC events. The combination 27% CC efficiency/11% residual NC (scenario "C" in Figure 27) corresponds to the most conservative scenario in which all CC ν_e events also producing a charged pion are rejected. The more optimistic value of 50% CC efficiency assumes that they can be partly recovered.

When a high-energy charged particle passes through the LSc, it creates a superposition of spherical light waves, forming a spherical backward running light front and a v-shaped forward light front resembling a Cherenkov cone, thus creating distinct arrival time patterns at the PMTs. Analyzing these patterns allows for a track reconstruction, as it has been shown for cosmic muons by KamLAND and Borexino. Recent studies investigate the capability of this method for ν event reconstruction with increasing sophistication and accuracy. Figure 28 shows example tracks from the reconstruction of muons and electrons obtained by an algorithm capable of producing density profiles for the light emission inside the scintillator. Due to the broader and shorter profile of the emerging electromagnetic shower, e and μ can be clearly distinguished.

Neutrino mixing parameters can also be determined in LENA using much shorter baselines. Based on high-intensity synchrotrons producing GeV protons, $\overline{\nu}_\mu$ from the decay of stopped π^+ can be used for an $\overline{\nu}_\mu \leftrightarrow \overline{\nu}_e$ appearance experiment at baselines of the order of several km. As it has been demonstrated in the DAEδALUS proposal [72], a configuration using sources at three different baselines provides sensitivity to both θ_{13} and δ_{CP}, a measurement largely complementary to the long-baseline option. Furthermore, intense radioactive electron capture sources placed on top or inside the detector can be used to search for sterile neutrino oscillations at wavelengths of several meters by the observation of a spatial oscillation pattern inside the detector [73].

Last but not least, neutrino physics is not the only field where LENA can improve our current knowledge of elementary physics. Due to its high target mass and the excellent background discrimination, LENA is capable of increasing the limit of the proton lifetime to $\tau_p \geq 4 \times 10^{34}$ years in the channel $p \rightarrow K^+\overline{\nu}$, based on 10 years of measurement [74].

The LENA detector and its implementation in the Pyhäsalmi mine is shown in Figure 24.

The *MEMPHYS* (Megaton Mass Physics) project is discussed here with particular interest for deployment in an extended Modane Laboratory (LSM: Laboratoire Souterrain de Modane France), the distance from CERN being optimal for a low-energy neutrino beam [75]. Due to the short distance to CERN, this experiment has an excellent reach for leptonic CP violation search. The experiment is based on one of the most understood techniques for neutrino detection: Cherenkov light emission in water by charged particles resulting from neutrino interactions. At beam energies below 1 GeV, the water Cherenkov technique is well adapted to the physics scope of LAGUNA. Each tank of MEMPHYS is about 10 times Super-Kamiokande, and therefore only a mild extrapolation from an existing detector is necessary.

The project aims at a fiducial mass around half a megaton obtained with 2 cylindrical detector modules of 65 meters in diameter and 103 meters in height. A schematic view is shown in Figure 29. It takes into account the need to have a veto volume, 1.5 m thick, plus a minimal distance of about 2 meters between photodetectors and interaction vertices, leaving a sufficient space for ring development and to protect from γ from the PMTs natural radioactivity. The fiducial volume

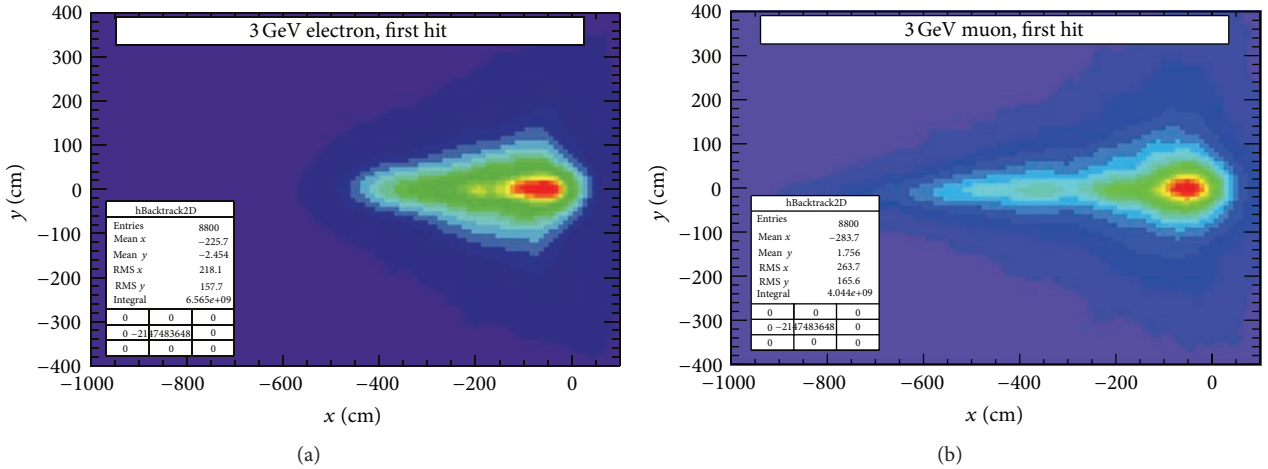

Figure 28: Visualization of the tracking for electron (a) and muon (b) events in LENA. The pictures show density profiles for the light emission inside the scintillator. Due to the broader and shorter profile of the emerging electromagnetic shower, e and μ can be clearly distinguished [70].

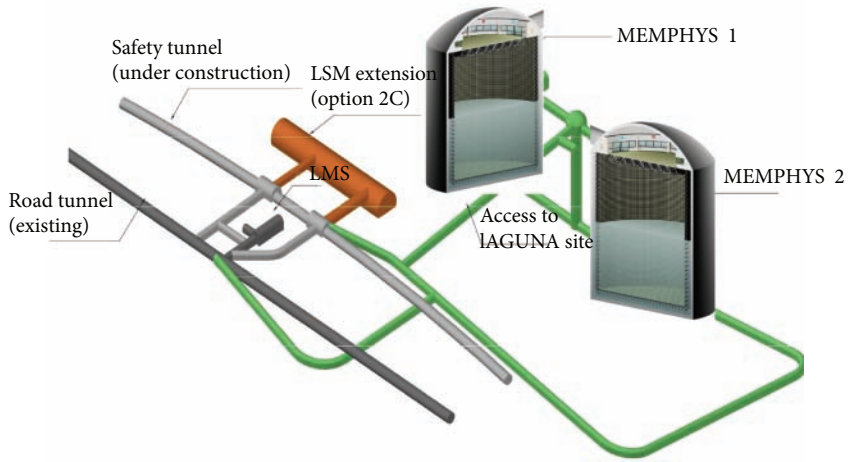

Figure 29: Possible layout for the future neutrino observatory at the Fréjus tunnel. The MEMPHYS detector is made of two independent tanks 60 m apart from each other. Each tank is 65 m in diameter and 103 m in height.

is 530 kilotons. The light sensors choice is to instrument the detector with photomultipliers tubes (PMTs) with a geometrical coverage of 30%. However, a number of technical aspects are under investigation. One of the challenges is the large number of photomultipliers required. The baseline design of MEMPHYS uses about 220,000 $8''$ PMTs.

For a MEMPHYS detector at the Fréjus site, situated at 130 km from CERN, the first peak of the neutrino oscillation probability occurs at a beam energy between 0.2 and 0.4 GeV. The sensitivity of the MEMPHYS experiment to CP violation is shown in Figure 30.

The deep underground position of the MEMPHYS neutrino observatory (4800 m.w.e.) allows a very rich nonaccelerator physics program. We summarize in Table 9 the results for nonaccelerator physics: the discovery potential of MEMPHYS for proton decay (90% CL in 10 years), the number of events for a supernova explosion at 10 kpc, the signal over background ratio for DSN neutrinos, and the rate of solar, atmospheric, and reactor neutrinos in the detector per year. We assume an energy threshold of 5 MeV. The improvement of the new, optimized design (2 tanks 65 m $\times$ 10^3 m) for the detector is shown in the right column.

The coverage of large area with PMTs at a "low" cost implies a readout integrated electronics circuit (called ASIC) for groups of PMT (matrix of 4×4). The development of such electronics is the aim of a dedicated French R&D program, called PMm^2 [76, 77]. The circuit under development allows to integrate for each group of PMTs: a high-speed discriminator on the signal photoelectron (ph.e), the digitization of the charge (on 12 bits ADC) to provide numerical signals, the digitization of time (on 12 bits TDC) to provide time information, a channel-to-channel gain adjustment, and a common high voltage. All the electronic and acquisition developed in the PMm^2 program is going to be fully tested with the MEMPHYNO prototype installed at the APC laboratory. MEMPHYNO is a test bench for any kind of light sensor

Table 9: Summary of nonaccelerator physics in MEMPHYS.

Topic	MEMPHYS (440 kt)	(~500 kt)
Proton decay:	In 10 years	In 10 years
$e^+\pi^0$	$<1.0 \times 10^{35}$ [y] 90% CL	$\sim 1.2 \times 10^{35}$ [y] 90% CL
$\overline{\nu}K^+$	$<2 \times 10^{34}$ [y] 90% CL	$\sim 2.4 \times 10^{34}$ [y] 90% CL
SN ν (10 kpc):		
CC	2.0×10^5 ($\overline{\nu}_e$)	$\sim 2.4 \times 10^5$ ($\overline{\nu}_e$)
ES	1.0×10^3 (e)	$\sim 1.2 \times 10^3$ (e)
DSN ν (S/B 5 y)	(43–109)/47 ($\star$)	(52–131)/57 ($\star$)
Solar ν		
^{8}B ES	1.1×10^6 per y	$\sim 1.3 \times 10^6$ per y
Atm. ν (per y)	4.0×10^4	$\sim 4.8 \times 10^4$
Geo ν	Needs 2 MeV thr.	Needs 2 MeV thr.
Reactor ν (per y)	6.0×10^4 ($\star$)	$\sim 7.2 \times 10^4$ ($\star$)

The ($\star$) stands for the case where Gd salt is added to the water of one tank. The values on the right column are an extrapolation of the left ones.

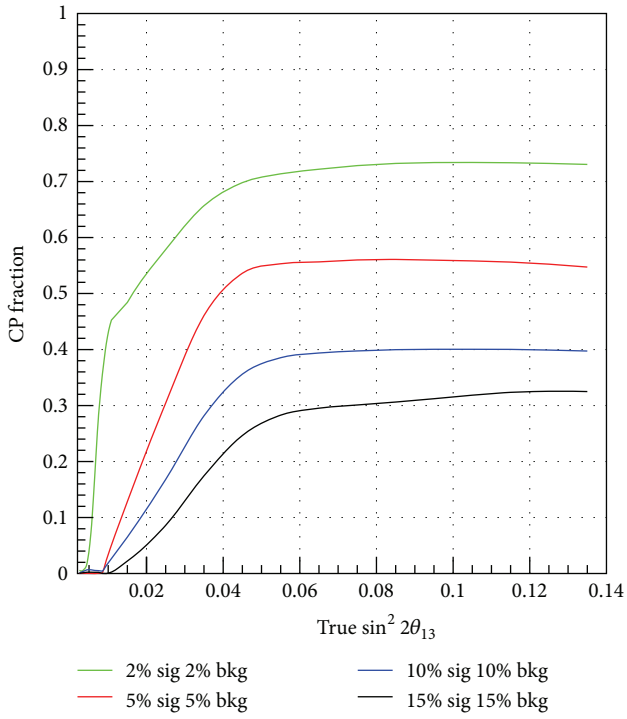

Figure 30: Sensitivity to leptonic CP violation of the MEMPHYS experiment at 3σ for different assumptions on the systematic error for the signal (sig) and the background (bkg). The evaluation is based on the CERN to Fréjus Superbeam with 2 years running in neutrino mode and 8 years running in anti-neutrino mode.

or electronics solution for next-generation megaton size experiments. This prototype is realized with a PEHD (polyethylene) tank of $2 \times 2 \times 2\,\mathrm{m}^3$ filled with water and a hodoscope made by 4 scintillator planes (kindly donated by the OPERA [78] collaboration)—2 on the top and 2 on the bottom— for the trigger of the incoming cosmic muons. A schematic view of the Memphyno tank with the muon hodoscope (green) and the PMm2 matrix (read dots) is shown in Figure 31(a). In Figures 31(b) and 31(c), the PMT matrix as well as the pressure resistant box for the electronics is shown.

The development on grouped electronics and photosensors is of very high interest for all the three detector options of the LAGUNA project. In particular the strong synergy with the LENA detector leads to a joint study within a collaborative effort between German and French groups [60].

In parallel to the development on photosensors and electronics, a large effort on the simulation of the detector performance is ongoing.

The neutrino event generator is based on GENIE [79] and the full simulation of the MEMPHYS detector is based on GEANT4 [80, 81]. The code has been developed starting from the Super-Kamiokande algorithm and adapted to the new geometry and PMT choice of MEMPHYS. A new event reconstruction algorithm for ring and vertex finding has been developed. Event reconstruction and analysis procedure have been essentially focalized on the reconstruction of the incoming neutrino energy and the identification of its flavor to perform appearance or disappearance analyses with the different types of beams. In order to properly take into account all the effects of the reconstruction, the detector performance has been conventionally described in terms of *"migration matrices"* representing the neutrino reconstructed energy versus the true one [82].

5. Conclusions

Neutrinos physics is one of the most dynamic and exciting fields of research in fundamental particle physics and astrophysics. The next-generation neutrino detector will address fundamental properties of the neutrino like mass hierarchy, the mixing angle θ_{13}, and the CP phase. We will enter the era of precision measurement of all elements of the Pontecorvo-Maki-Nakagawa-Sakata (PMNS) matrix. A new deep underground neutrino observatory will allow neutrino astronomy with solar, atmospheric, and supernova neutrinos as well as the detection of geo-neutrinos in the case of the LENA detector. Such a new detector naturally allows for major improvements in the search for nucleon decay. A

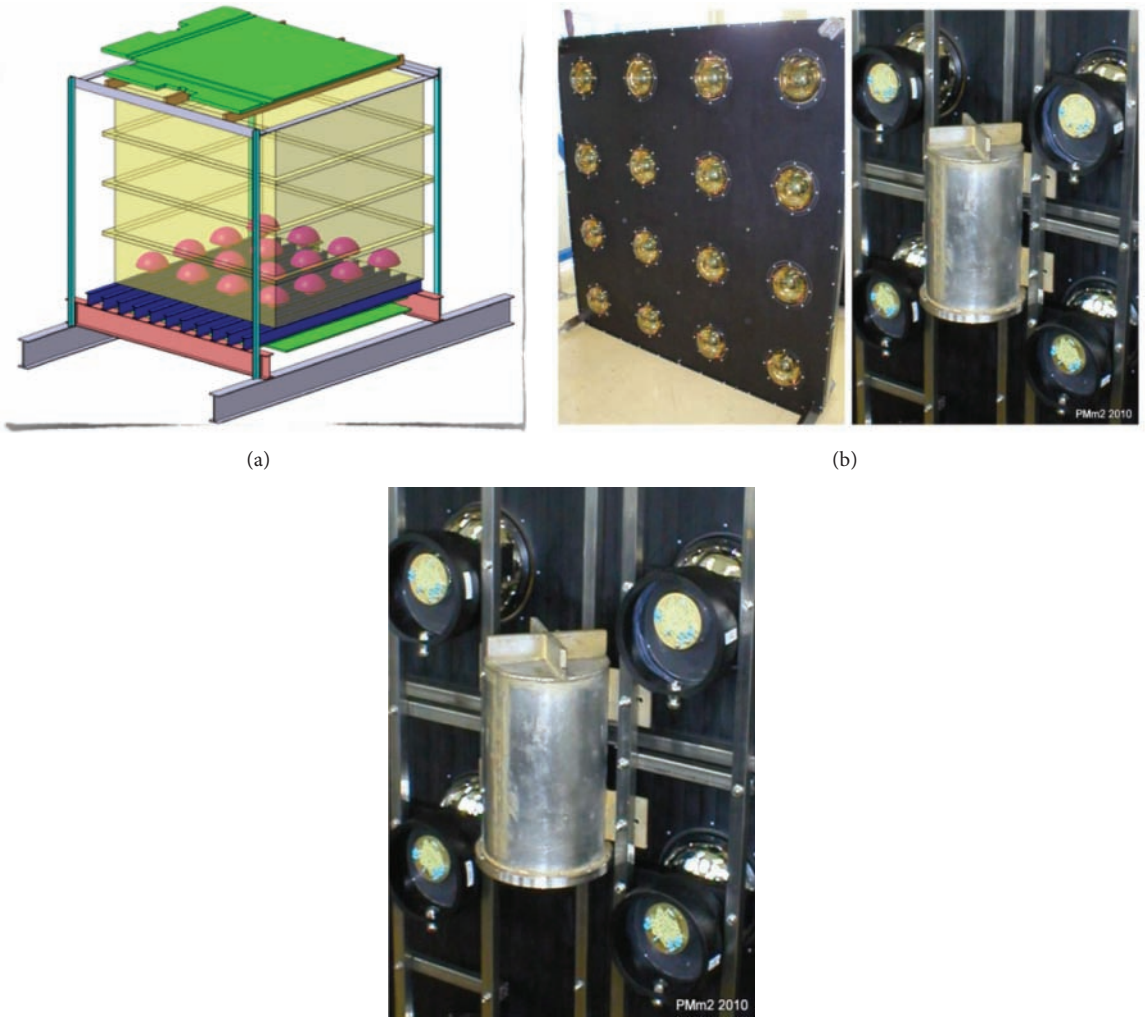

(a) (b)

(c)

Figure 31: (a) Schematic view of the MEMPHYNO prototype. (b) Photograph of the PMm2 matrix of 16 8″ Hamamatsu PMTs. (c) Backside of the matrix showing the watertight box for the electronics.

next-generation neutrino observatory needs a huge, megaton scale detector which in turn has to be installed in a new, international underground laboratory, capable of hosting such a huge detector.

Acknowledgments

The authors are grateful to the European Commission for the financial support of the project through the FP7 Design Studies LAGUNA (Project no. 212343), LAGUNA-LBNO (Project no. 284518), and EUROnu (Project no. 212372). The EC is not liable for any use that may be made of the information herein. They thank the French Centre National de Recherche Scientifique for the support of the project in form of the PICS. They are also grateful to the Japan Society for the Promotion of Science Grants-in-Aid for Scientific Research (Grant no. 23244058). This work was partially supported by the US Department of Energy.

References

[1] A. Badertscher, T. Hasegawa, T. Kobayashi et al., "A possible future long baseline neutrino and nucleon decay experiment with a 100 kton liquid argon TPC at Okinoshima using the J-PARC neutrino facility," http://arxiv.org/abs/0804.2111. In press.

[2] K. Abe, T. Abe, H. Aihara et al., "Letter of intend: the hyper-kamiokande experiment—detector design and physics potential," http://arxiv.org/abs/1109.3262. In press.

[3] P. Adamson, C. Andreopoulos, R. Armstrong et al., "Measurement of the neutrino mass splitting and flavor mixing by MINOS," *Physical Review Letters*, vol. 106, Article ID 181801, 2011, http://arxiv.org/abs/1103.0340.

[4] D. S. Ayres, G. R. Drake, M. C. Goodman et al., "The NOvA technical design report," Fermilab Design 2007-01, 2007.

[5] K. S. McFarland and MINERvA Collaboration, "MINERνA: a dedicated neutrino scattering experiment at NuMI," *Nuclear Physics B*, vol. 159, pp. 107–112, 2006.

[6] A. A. Aguilar-Arevalo, C. E. Anderson, and L. M. Bartoszek, "The MiniBooNE detector," *Nuclear Instruments and Methods in Physics Research Section A*, vol. 599, no. 1, pp. 28–46, 2009.

[7] H. Chen, J. Farrell, F. Lanni et al., "Proposal for a new experiment using the booster and NuMI neutrino beamlines: MicroBooNE," FERMILAB-PROPOSAL-0974, 2007.

[8] K. N. Abazajian, M. A. Acero, S. K. Agarwalla et al., "Light sterile neutrinos: a white paper," http://arxiv.org/abs/1204.5379. In press.

[9] W. J. Marciano, "Extra long baseline neutrino oscillations and CP violation," http://arxiv.org/abs/hep-ph/0108181. In press.

[10] M. V. Diwan, D. Beavis, M.-C. Chen et al., "Very long baseline neutrino oscillation experiments for precise measurements of mixing parameters and CP violating effects," *Physical Review D*, vol. 68, Article ID 012002, 2003.

[11] The US long-baseline study report, all associated documents, presentations, plots, studies, spectra, http://www.phy.bnl.gov/~diwan/nwg/fnal-bnl, Fermilab-0801-AD-E, BNL-77973-2007-IR, http://arxiv.org/abs/0705.4396.

[12] M. V. Diwan, "The Case for a super neutrino beam," *Frascati Physics Series*, vol. 35, pp. 89–109, 2004, http://arxiv.org/abs/quant-ph/0407047.

[13] National Research Council Report, *Neutrinos and Beyond, New Windows on Nature*, National Acedemy Press, 2003.

[14] National Research Council, *An Assessment of the Science Proposed for the Deep Underground*, Science and Engineering Laboratory (DUSEL), National Research Council, National Academy Press, 2011.

[15] Neutrino Scientific Assessment Group, *Recommendation to the Department of Energy and the National Science Foundation on the Future U.S. Program in Neutrino Oscillations*, Neutrino Scientific Assessment Group, 2007.

[16] Report of the Particle Physics Projects Prioritization Panel, *U.S. Particle Physics: Scientific Opportunities. A Strategic Plan for the Next Ten Years*, 2008.

[17] F. P. An, J. Z. Bai, H. R. Band et al., "Observation of electron-antineutrino disappearance at Daya Bay," *Physical Review Letters*, vol. 108, no. 17, Article ID 171803, 2012.

[18] S. Nagaitsev, "Project X—a new multi-megawatt proton source at Fermilab," Tech. Rep. FERMILABCONF- 11-092-AD, 2011.

[19] The Conceptual Design Report for LBNE is available from Fermilab, http://lbne.fnal.gov/reviews/CD1-review-top.shtml#DesignDocuments.

[20] A. Bernstein, M. Bishai, E. Blucher et al., "Report on the depth requirements for a massive detector at homestake," http://arxiv.org/abs/0907.4183. In press.

[21] http://www.fnal.gov/directorate/lbne reconfiguration/.

[22] M. Bishai, M. V. Diwan, S. Kettell et al., "Neutrino oscillations in the precision era," http://arxiv.org/abs/1203.4090.

[23] T. Akiri, D. Allspach, M. Andrews et al., "The 2010 interim report of the long-baseline neutrino experiment collaboration physics working groups," http://arxiv.org/abs/1110.6249.

[24] P. Huber, J. Kopp, M. Lindner, and W. Winter, "GLoBES: general long baseline experiment simulator," PoS NUFACT 08, 145, 2008.

[25] K. Abe, N. Abgrall, Y. Ajima et al., "Indication of electron neutrino appearance from an accelerator-produced off-axis muon neutrino beam," *Physical Review Letters*, vol. 107, Article ID 041801, 2011.

[26] Y. Abe, C. Aberle, T. Akiri et al., "Indication of reactor $\overline{\upsilon}_e$ disappearance in the double Chooz experiment," *Physical Review Letters*, vol. 108, no. 13, Article ID 131801, 7 pages, 2012.

[27] F. P. An, J. Z. Bai, A. B. Balantekinet et al., "Observation of electron-antineutrino disappearance at Daya Bay," *Physical Review Letters*, vol. 108, no. 17, Article ID 171803, 7 pages, 2012.

[28] J. K. Ahn, S. Chebotaryov, J. H. Choi et al., "Observation of reactor electron antineutrinos disappearance in the RENO experiment," *Physical Review Letters*, vol. 108, no. 19, Article ID 191802, 6 pages, 2012.

[29] K. Abeaw, N. Abgrallp, H. Aihara et al., "The T2K experiment," *Nuclear Instruments and Methods in Physics Research A*, vol. 659, no. 1, pp. 106–135, 2011.

[30] T. Hasegawa, "Introductory remark on the first international workshop towards the giant liquid argon charge imaging experiment (GLA2010)," *Journal of Physics*, vol. 308, Article ID 012001, 2011.

[31] D. Dwyer and Daya Bay collaboration, "Daya Bay results," in *Proceedings of the 25th International Conference on Neutrino Physics and Astrophysics*, Kyoto, Japan, June 2012.

[32] M. Yoshioka, T. Hasegawa, O. Hirabayashi et al., "Okinoshima site study," *Journal of Physics*, vol. 308, no. 1, Article ID 012028, 2011.

[33] A. Bueno, Z. Dai, Y. Ge et al., "Nucleon decay searches with large liquid Argon TPC detectors at shallow depths: atmospheric neutrinos and cosmogenic backgrounds," *Journal of High Energy Physics*, vol. 0704, article 041, 2007.

[34] "EUROnu—A High Intensity Neutrino Oscillation Facility in Europe," FP7- INFRASTRUCTURES-2007-1, ref. 212372.

[35] F. Gerigk et al., "Conceptual design of the SPL II: A high-power superconducting H-linac at CERN," *CERN* , 104 pages, 2006.

[36] A. de Bellefon, J. Bouchez, J. Busto et al., "MEMPHYS: a large scale water Cherenkov detector at Frejus," http://arxiv.org/abs/hepex/0607026.

[37] https://www.ids-nf.org/wiki/FrontPage/Documentation/IDR.

[38] I. Efthymiopoulos, C. Hessler, H. Gaillard et al., "HiRadMat: a new irradiation facility for material testing at CERN," in *Proceedings of the 2nd International Particle Accelerator Conference*, p. TUPS058, San Sebastian, Spain, September 2011.

[39] A. Pardons et al., "Horn Operational Experience in K2K, MiniBooNE, NuMI and CNGS," in *Proceedings of the 10th International Workshop on Neutrino Factories, Superbeams and Betabeams*, p. 96, Valencia, Spain, June 2008.

[40] M. Bogomilov et al., "The MICE Muon Beam on ISIS and the beam-line instrumentation of the muon ionization coolingexperiment," http://arxiv.org/abs/1203.4089.

[41] K. Yonehara, "Recent progress of RF Cavity Study at mucool test area," http://arxiv.org/ftp/arxiv/papers/1201/1201.5903.pdf.

[42] R. Barlow et al., "EMMA: the worlds first non-scaling FFAG," *Nuclear Instruments and Methods in Physics Research A*, vol. 624, pp. 1–19, 2010.

[43] P. Zucchelli, "A novel concept for a $\overline{\upsilon}_e/\upsilon_e$ neutrino factory: the beta beam," *Physics Letters B*, vol. 532, pp. 166–172, 2002.

[44] M. Benedikt et al., "Conceptual design report for a Beta-Beam facility," *The European Physical Journal A*, vol. 47, article 24, 2011.

[45] C. Rubbia, A. Ferrari, Y. Kadi et al., "Beam cooling with ionisation losses," *Nuclear Instruments and Methods in Physics A*, vol. 568, pp. 475–487, 2006.

[46] L. Arnaudon et al., "The LINAC4 Project at CERN," in *Proceedings of the 2nd International Particle Accelerator Conference*, San Sebastian, Spain, September 2011.

[47] K. Habig, "MINOS neutrino oscillation results," *Journal für die Reine und Angewandte Mathematik*, vol. 668, pp. 149–190, 2012.

[48] E. Fernandez-Martinez, P. Coloma, and P. Hernandez, "Physics comparison: future facilities in Europe and elsewhere," in *Proceedings of the 4th Annual EUROnu Meeting*, Paris, France, June 2012.

[49] S. Fukuda, Y. Fukudaa, T. Hayakawa et al., "The superkamiokande detector," *Nuclear Instruments and Methods in Physics Research Section A*, vol. 501, article 418, 2003.

[50] "ASPERA," http://www.aspera-eu.org.

[51] W. D. Arnett and J. L. Rosner, "Neutrino mass limits from SN1987a," *Physical Review Letters*, vol. 58, article 1906, 1987.

[52] K. S. Hirata, T. Kajita, M. Koshiba et al., "Observation in the Kamiokande-II detector of the neutrino burst from supernova SN, 1987a," *Physical Review D*, vol. 38, pp. 448–458, 1988.
[53] Laguna FP7 design study, Grant Agreement 212343.
[54] D. Autiero, J. Aysto, A. Badertscher et al., "Large underground, liquid based detectors for astro-particle physics in Europe: scientific case and proposals," *Journal of Cosmology and Astroparticle Physics*, vol. 0711, Article ID 011, 2007.
[55] T. Patzak et al., "LAGUNA: future megaton detectors in Europe," *Journal of Physics*, vol. 309, Article ID 012022, 2011.
[56] LAGUNA-LBNO FP7 design study, Grant agreement 284518.
[57] A. Rubbia, "Underground neutrino detectors for particle and astroparticle science: the Giant Liquid Argon Charge Imaging ExpeRiment (GLACIER)," *Journal of Physics*, vol. 171, Article ID 012020, 2009.
[58] L. Oberauer, F. von Feilitzsch, and W. Potzel, "A large liquid scintillator detector for low-energy neutrino astronomy," *Nuclear Physics*, vol. 138, pp. 108–111, 2005.
[59] J. L. Borne, J. Busto, J.-E. Campagne et al., "The MEMPHYS project," *Nuclear Instruments and Methods in Physics Research Section A*, vol. 639, pp. 287–289, 2011.
[60] PICS (Projet international de cooperation scientifique) Grant Agreement 5226.
[61] A. Rubbia, "Future liquid Argon detectors," in *Proceedings of the 25th International Conference on Neutrino Physics and Astrophysics*, Kyoto, Japan, June 2012.
[62] A. Stahl, C. Wiebusch, A. M. Guler et al. et al., "Expression of interest for a very long baseline neutrino oscillation experiment (LBNO)," Tech. Rep. CERN-SPSC-2012-021, SPSC-EOI-007, 2012.
[63] A. Rubbia, "Underground neutrino detectors for particle and astroparticle Science: the Giant Liquid Argon Charge Imaging ExpeRiment (GLACIER)," *Journal of Physics*, vol. 171, Article ID 012020, 2009.
[64] M. Wurm, F. John Beacom, B. Leonid Bezrukov et al., "The next-generation liquid-scintillator neutrino observatory LENA," *Astropart Physics*, vol. 35, pp. 685–732, 2012.
[65] M. Wurm, B. Caccianiga, D. D'Angelo et al., "Search for modulations of the solar Be-7 ux in the next-generation neutrino observatory LENA," *Physical Review D*, vol. 83, Article ID 032010, 2011.
[66] C. Hagner, "LENA-Low Energy Neutrino Astronomy," in *Proceedings of the Neutrino Town Meeting, CERN*, May 2012.
[67] M. Wurm, F. von Feilitzsch, M. Göger-Neff et al., "Detection potential for the diffuse supernova neutrino background in the large liquid-scintillator detector LENA," *Physical Review D*, vol. 75, Article ID 023007, 2007.
[68] K. A. Hochmuth, F. V. Feilitzsch, B. D. Fields et al., "Probing the Earths interior with a large-volume liquid scintillator detector," *Astroparticle Physics*, vol. 27, pp. 21–29, 2007.
[69] S. T. Petcov and T. Schwetz, "Precision measurement of solar neutrino oscillation parameters by a long-baseline reactor neutrino experiment in Europe," *Physics Letters B*, vol. 642, pp. 487–494, 2006.
[70] Private communication from K. Loo, Department of Physics, University of Jyväskylä, Finland.
[71] P. Coloma, T. Li, and S. Pascoli, "Long-baseline super-beam experiments in Europe within LAGUNA," http://arxiv.org/abs/1110.1402.
[72] J. Alonso, F. T. Avignone, W. A. Barletta et al., "Expression of interest for a novel search for CP violation in the neutrino sector: DAEdALUS," http://arxiv.org/abs/1006.0260.
[73] N. Yu. Novikov, T. Enqvist, A. N. Erykalov et al., "Neutrino oscillometry at the next generation neutrino observatory," http://arxiv.org/abs/1110.2983.
[74] T. Marrodán Undagoitia, von Feilitzsch, M. Goger-Neff et al., "Search for the proton decay $P \rightarrow K^+$ anti-nu in the large liquid scintillator low energy neutrino astronomy detector LENA," *Physical Review D*, vol. 72, Article ID 075014, 2005.
[75] J.-E. Campagne, M. Maltoni, M. Mezzetto et al., "Physics potential of the CERN-MEMPHYS neutrino oscillation project," *Journal of High Energy Physics*, vol. 704, Article ID 003, 2007.
[76] B. Genolini, P. Barrillon, S. Blin et al., "PMm**2: large photomultipliers and innovative electronics for the next-generation neutrino experiments," *Nuclear Instruments and Methods in Physics A*, vol. 610, pp. 249–252, 2009.
[77] J. E. Campagne, S. Conforti Di Lorenzo, S. Drouet et al., "PMm**2: R&D on trigger less acquisition for the next generation neutrino experiments," *JINST*, vol. 6, 2011.
[78] OPERA Proposal, CERN/SPSC, 2000-028, SPSC/P318, LNGS P25/2000.
[79] C. Andreopoulos, A. Bell, D. Bhattacharya et al., "The GENIE neutrino monte carlo generator," *Nuclear Instruments and Methods A*, vol. 614, pp. 87–104, 2010.
[80] S. Agostinelli, J. Allison, K. Amako et al., "GEANT4: a simulation toolkit," *Nuclear Instruments and Methods A*, vol. 506, pp. 250–303, 2003.
[81] J. Allison, K. Amako, Apostolakis, J et al., "GEANT4 developments and applications," *IEEE Transactions on Nuclear Science*, vol. 53, pp. 270–278, 2006.
[82] L. Agostino, M. Buizza-Avanzini, M. Dracos et al., "Study of the performance of a large scale water-Cherenkov detector (MEMPHYS)," http://arxiv.org/abs/1206.6665.

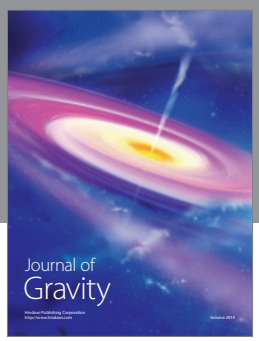

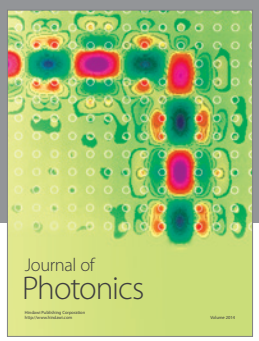

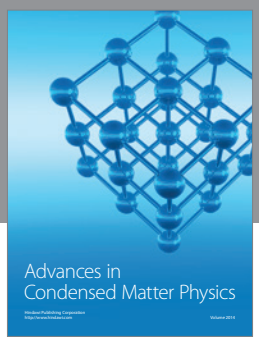

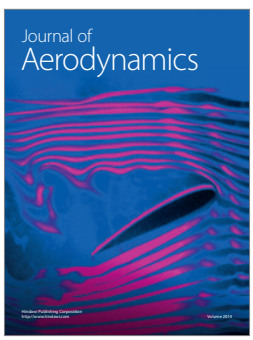

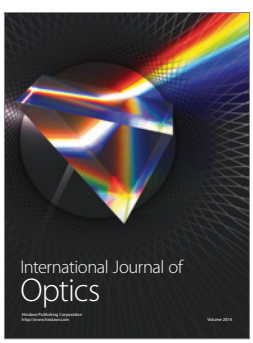

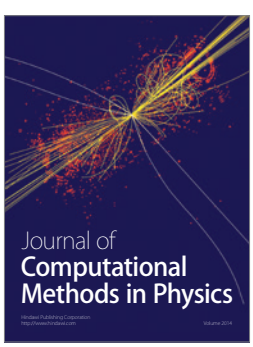

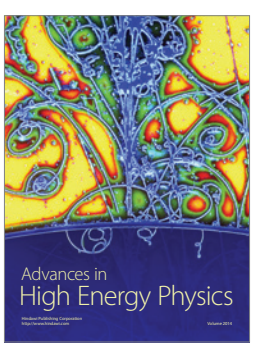

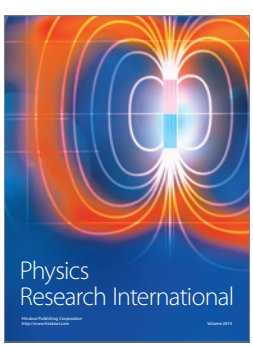

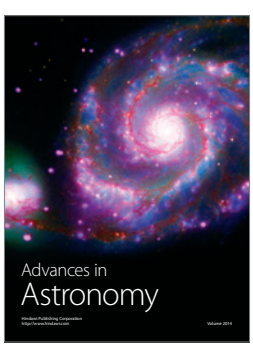

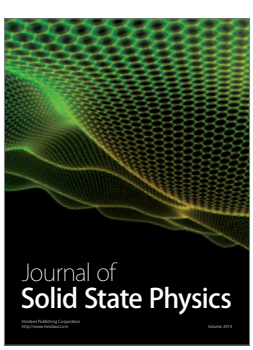

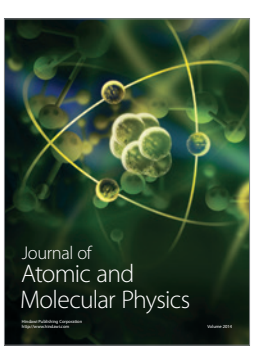

Hindawi

Submit your manuscripts at
http://www.hindawi.com